Eur. J. Immunol. 2010. 40: 1–7 DOI 10.1002/eji.200939479 Clinical immunology

European Journal of Immunology

Inhibition of HIV replication by a CD4-reactive Fab of an IgM clone isolated from a healthy HIV-seronegative individual

Makiko Hamatake[1], Jun Komano[1], Emiko Urano[1], Fumiko Maeda[2], Yasuko Nagatsuka[3] and Masataka Takekoshi[2]

[1] AIDS Research Center, National Institute of Infectious Diseases, Tokyo, Japan
[2] Department of Molecular Life Science, Division of Basic Molecular Science and Molecular Medicine, Tokai University School of Medicine, Isehara, Japan
[3] Hirabayashi Research Unit, Brain Science Institute, RIKEN, Wako, Saitama, Japan

HIV replication is restricted by some anti-CD4 mouse mAb *in vitro* and *in vivo*. However, a human monoclonal anti-CD4 Ab has not been isolated. We screened EBV-transformed peripheral B cells from 12 adult donors for CD4-reactive Ab production followed by functional reconstitution of Fab genes. Three independent IgM Fab clones reactive specifically to CD4 were isolated from a healthy HIV-seronegative adult (~0.0013% of the peripheral B cells). The germ line combinations for the VH and VL genes were VH3-33/L6, VH3-33/L12, and VH4-4/L12, respectively, accompanied by somatic hypermutations. Genetic analysis revealed a preference for V-gene usage to develop CD4-reactive Ab. Notably, one of the CD4-reactive clones, HO538-213, bearing 1×10^{-8} M dissociation constant (Kd) to recombinant human CD4, limited the replication of R5-tropic and X4-tropic HIV-1 strains at 1–2.5 μg/mL in primary mononuclear cells. This is the first clonal genetic analysis of human monoclonal CD4-reactive Ab. A mAb against CD4 isolated from a healthy individual could be useful in the intervention of HIV/AIDS.

Key words: Autoimmunity · CD4-reactive Ab · IgM · Inhibition of HIV replication

Supporting Information available online

Introduction

CD4 is a T-cell marker that serves as a principal receptor for HIV. CD4-reactive Ab are detected in HIV-infected individuals (~13%) [1, 2] and HIV-exposed seronegative individuals (34%) [3]. In addition, some healthy individuals are positive for anti-CD4 Ab (~0.6%) [4]. Replication of multiple HIV clades is blocked by mouse mAb against CD4 *in vitro* and *in vivo* [5–12]. Thus, it is possible that anti-CD4 Ab play a role in protecting individuals from HIV infection and delaying AIDS disease progression. Similar arguments have been made for Ab against CCR5, a coreceptor for HIV [3, 10, 13]. Furthermore, some clinical studies suggest that CD4-reactive Ab, including a humanized mAb, has therapeutic potential against HIV infection and AIDS progression [5, 8, 10, 12]. However, the development and pathophysiological roles of self-recognizing Ab in healthy individuals are still largely unknown, and a human mAb against CD4 has not yet been isolated.

To gain insights into the genesis of auto-reactive Ab and to characterize the nature of CD4-reactive auto-Ab, we conducted experiments to isolate human monoclonal anti-CD4 Ab from PBMC of 12 HIV-seronegative adult donors. We succeeded in isolating three independent IgM clones recognizing CD4 from a healthy donor. Analysis of the V-region sequences of CD4-reactive Ab

Correspondence: Dr. Jun Komano
e-mail: ajkomano@nih.go.jp

revealed a preference for V gene usage to give rise to CD4-reactive Ab. This is the first report describing CD4-reactive human mAb.

Results and discussion

Isolation of CD4-reactive IgM clones from a healthy individual

PBMC were collected from 12 HIV-seronegative adult volunteers, including two healthy and ten with autoimmune disorders, and B-lymphoblastoid cell lines (B-LCL) were established by infecting the cells with EBV (for experimental procedure, see Supporting Information Fig. 1). B-LCL were propagated in oligoclonal pools. In 790 cultures from one healthy donor, we identified two cultures positive for recombinant human CD4 (rhCD4) reactivity, HO538 and HO702, using ELISA (Fig. 1A). This donor may have a unique Ab repertoire, as auto-reactive B-LCL cultures were identified significantly more frequently in this donor than in the others (Fig. 1A). The rhCD4 reactivity was specific, as no binding was observed to 72 other viral, bacterial, and auto-Ag screened in parallel (Supporting Information Fig. 2). We amplified the Ig genes encoding Fab regions by RT-PCR and cloned them into the bacterial expression vector pFabI-His2 that produces Fab fragments of an inserted set of VH and VL genes. We expected that some clones should reconstitute the CD4-reactive Fab present in the original B-LCL cultures. After screening by ELISA, one CD4-reactive Fab clone, HO538-213, was isolated from the HO538 culture, and two independent clones, HO702-001 and HO702-016, were isolated from the HO702 culture. These Fab clones originated from IgM, as determined by the sequence analysis. The estimated efficiency of peripheral B cells producing CD4-reactive Ab was ~0.0013% (three clones/2.4×10^5 estimated screened B cells × 100 (%), given that the B cells compose 10% of PBMC and that EBV immortalization is 30% efficient on average) [14]. According to the ELISA data, the Fab concentrations that yielded 50% maximal binding were ~8 μg/mL for HO538-213, and ~1 μg/mL for HO702-001 and HO702-016 (Fig. 1B). Consistent with these data, the BIACORE assay revealed that the dissociation constant (Kd) of HO538-213, HO702-001, and HO702-016 to rhCD4 was 6.5×10^{-8}, 7.7×10^{-9}, and 2.7×10^{-9} M, respectively (Fig. 1C), which is relatively weak compared with average Ab–Ag interactions (*e.g.* the Kd of mouse mAb Leu-3a to rhCD4 is 2.2×10^{-10} M).

Genetic analysis of CD4-reactive IgM clones

The Fab sequences were analyzed by the Kabat database (http://www.ncbi.nlm.nih.gov/igblast/) in GenBank, as previously described [15, 16]. The Ig gene family of each gene and the most homologous germ line are indicated (Fig. 2A). All the three clones were of the IgM class and had a κ-chain for VL. Comparison of the

A

Donor	Number of tested cultures	CD4	Nuclear antigen	Blood type i-glycolipid
Healthy 1	790	2 (0.3%)*	21 (2.6%)*	28 (3.5%)*
Healthy 2	160	0	0	0
Autoimmune (10 individuals)	435	0	3 (0.7%)	0

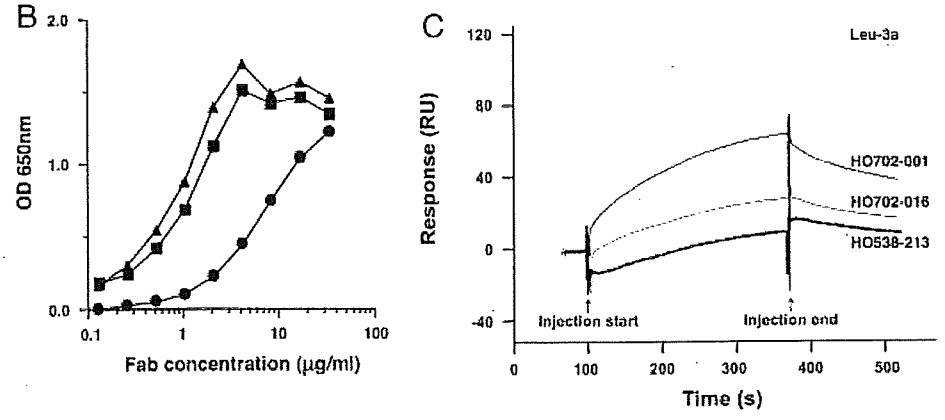

Figure 1. Isolation and characterization of healthy human-derived CD4-reactive Ab. (A) Summary of the frequency of B-LCL cultures that reacted to representative auto-Ag. The number of cultures positive for rhCD4 reactivity, HeLa cell nuclear staining, and blood type i-glycolipid are shown. *$p<0.05$, compared with other donor groups, Fisher's exact test. (B) CD4-binding kinetics of CD4-reactive IgM Fab. Serial dilutions of HO538-213 (circles), HO702-001 (triangles), and HO702-016 (squares) were incubated in microtiter plates pre-coated with rhCD4. (C) Surface plasmon resonance analysis of CD4-reactive IgM FAb HO702-001 (black), HO702-016 (dark gray), HO538-213 (bold), and mAb Leu-3a (gray) binding to immorbilized rhCD4. The concentration of Ab was 0.3 μg/mL, flow rate 20 μL/min, and reaction time 270 s. RU, resonance units.

heavy chain with the germ lines revealed that the μ-chains of HO538-213 and HO702-001 were 95 and 97% homologous to germ line VH 3-33, respectively, while HO702-016 was 96% homologous to germ line VH 4-4 [17]. For the light chains, the κ-chain Vkappa3 of HO538-213 was 97% homologous to germ line L6 [6, 18, 19], and κ-chain Vkappa1 of both HO702-001 and HO702-016 was 97% homologous to the germ line L12 [6, 18, 19]. These data suggest that there is a preferential use of VH and VL genes to develop CD4-reactive Ab, considering the number of VH and VL genes present before the Ig gene rearrangement. According to the sequence analysis, the VH amino acid sequences of HO538-213 and HO702-001 carried distinct mutations, although both were derived from the same germ line VH3-33. The mutations were more frequent in the CDR regions (Fig. 2B and C, Supporting Information Fig. 3), which is characteristic of somatic hypermutation (sHM) associated with affinity maturation. Unlike most sHM, however, mutations involving G/C were not dominant.

A

Clone	Ig class	VH family	Closest germline	% identity	VL family	Closest germline	% identity
HO538-213	IgM	VH 3	VH3-33	95%	Vk3	L6	97%
HO702-001	IgM	VH 3	VH3-33	97%	Vk-1	L12	97%
HO702-016	IgM	VH 4	VH4-4	96%	Vk-1	L12	97%

B

Clone			Number of mutations associated with: A	G	C	T	Ins[a]	del[a]	GC involvement [%][b]	Total	aa changes[c]	[%]
HO702-001	heavy chain	FR	3	2	1	0	0	0	50.0	6	2	33.3
		CDR	0	0	0	0	5	0	0.0	5	0	0.0
	light chain	FR	0	0	5	2	0	0	0.0	2	1	50.0
		CDR	1	0	0	0	6	0	0.0	7	0	0.0
		Total	4	2	1	2	11	0	50.0	20	3	15.0
HO702-016	heavy chain	FR	1	0	0	0	0	0	0.0	1	0	0.0
		CDR	0	2	1	0	11	0	100.0	8	0	0.0
	light chain	FR	0	0	0	2	0	0	0.0	2	1	50.0
		CDR	1	0	0	0	6	0	0.0	7	0	0.0
		Total	2	2	1	2	17	0	47.5	23	1	4.2
HO538-213	heavy chain	FR	2	1	1	4	0	0	25.0	8	3	37.5
		CDR	2	2	3	1	10	0	70.0	23	5	22.0
	light chain	FR	1	2	1	0	0	0	75.0	4	3	75.0
		CDR	3	1	2	0	2	0	28.0	6	3	50.0
		Total	8	6	7	6	17	0	60.0	43	13	30.2

C

Light chain

```
                    FR1                     CDR1          FR2           CDR2
HO538-213   ETVMTQSPATLSLSPGERATLSC  RASQSVNNYLA  WYQQRPGQAPSLLIY  DASNRAT
HO702-001/016 D-QL----S---A-V-D-V-IT-  -----ISSW--  ----K--K--K----  X--SLES

                    FR3                     CDR3          FR4
HO538-213   GIPARFSGSGSGTDFTLTISSLEPEDFAVYYC  QQ.RG.NWPHT  FGQGTKLEIKRT
HO702-001/016 -V-S---------E--------Q-D---I---  --YNSYSRIY-  ------------
```

Heavy chain

```
                    FR1                     CDR1          FR2           CDR2
HO538-213   QVQLVQSGGGVVQPGRSLRLSCA.ASG.FTFS  SYGMH  WVRQAPGKGLEWVA  VVCYDGRTTYYADSVKG
HO702-001   ----QEW-------------------------  -----  --------------  -IN---SNK--------
HO702-016   ----QE--P-L-K-SQT-S-T-TVSG-SISSG  --YWS  -I--PA------IG  RI-TSGS-N NP-L-S

                    FR3                     CDR3          FR4
HO538-213   RFTISRDISENTLYLQMNSLRAEDTAVYYCAK  DLNKGYCNNGGCYG.VDC  WGQGTLVTVSS
HO702-001   -------N-K---------------------R  -..RD.-SG-S--SWF-P  ----------
HO702-016   -V--SV-T-K-QFS-KLS-VT-A--------R  T.-PTL.GR-L.F...-Y  ----------
```

Figure 2. Genetic analysis of CD4-reactive Ab. (A) Summary of the Ig class, V-gene family, closest germ line, and percentage identity of the closest germ line of CD4-reactive Ab. (B) The mutation profiles of the CD4-reactive IgM Fab fragments. (C) The deduced protein sequences of the VH and VL genes of the CD4-reactive Fab fragments are aligned. FR, framework region. Dashes and dots indicate identical residues and deletions, respectively. See Supporting Information Fig. 2 for further detail.

Inhibition of HIV replication by a Fab fragment of a CD4-reactive IgM

We next examined the potential impact of these CD4-reactive Fab Ab on HIV replication. Viral replication was monitored in PBMC by measuring $p24^{CA}$ viral Ag levels in the culture supernatant. Among the three IgM Fab clones, HO538-213 suppressed R5-tropic virus HIV-1_{JR-FL} replication by 3.5±1.5-fold at 1–2.5 μg/mL (average±SD from four independent experiments, Fig. 3A). There was a modest but consistent suppression of X4-tropic virus HIV-1_{HXB2} replication (1.4±0.2-fold, average±SD from three independent experiments). A BIACORE and ELISA revealed that HO538-213 did not compete with the anti-CD4 mAb Leu-3a [20, 21] for CD4 binding. Leu-3a restricts HIV-1 replication by physically blocking *Env*-CD4 interaction (data not shown), suggesting that the epitope recognized by HO538-213 is distinct from the *Env*-interacting domain of CD4 [7, 22, 23]. The monoclonal anti-CD4 Ab OKT4a does not block *Env*-CD4 interaction, but restricts HIV-1 infection, although decreasing CD4 lateral diffusion on the cell surface [24–26]. We hypothesized that HO538-213 may have a similar mechanism of action. CD4 localizes to lipid rafts, and CD4-crosslinking activates signal transduction involving tyrosine kinases [27–29]. Thus, we treated MOLT-4 cells with HO538-213, and the lipid raft fraction was isolated by a membrane floatation assay as verified by the raft markers glycosphyngomyelin 1 and sphingomyelin (Fig. 3B, left panel). Tyrosine kinase activitiy was examined by immunoblotting, the lipid raft fractions using a PY20 anti-phosphotyrosine mAb (Fig. 3B, right panel, arrowhead). We detected a significant amount of tyrosine phosphorylation in the lipid raft fraction after HO538-213 treatment, indicating that HO538-213 can assemble cell surface CD4. This is consistent with our hypothesis that HO538-213 inhibits HIV-1 infection by decreasing the lateral movement of cell surface CD4.

Does CD4-reactive IgM function as a natural HIV resistance factor?

We then further characterized the donor from which the CD4-reactive Ab was isolated. The donor serum did not show a strong reactivity to rhCD4 at 1:10 dilution, where the non-specific effect was no longer detected. We analyzed the HIV-inhibition titer of the donor plasma. In a TZM-bl cell assay, the plasma did not block HIV replication at 1:50 dilution (data not shown). These data suggest that the CD4-reactive IgM circulates at very low titers in the donor and may not be sufficient to block HIV infection *in vitro*. However, it is possible that the CD4-reactive IgM may be able to limit HIV-1 propagation under *in vivo* conditions.

We next investigated the immunological status of the donor. IgG and IgM levels were within the normal range, and the plasma was negative for rheumatoid factor, anti-DNA, and anti-ribonucleoprotein Ab. However, the donor serum reacted to nuclear Ag at a titer of 1:160 (1:40 or less is considered normal), and the staining patterns were nucleolar (1:160) and speckled (1:80). Consistent with these data, the frequency of auto-reactive

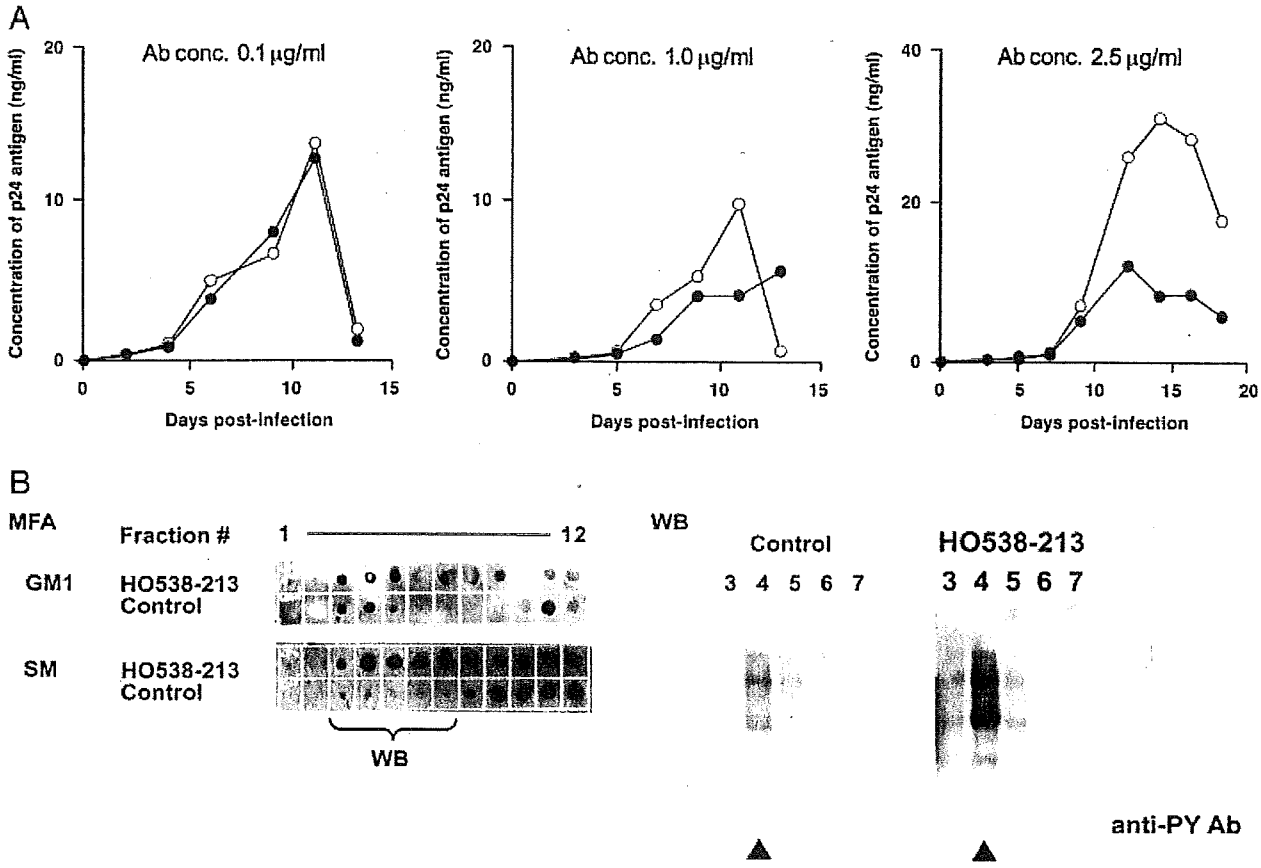

Figure 3. The effect of CD4-reactive Fab clone HO538-213 on HIV-1 replication. (A) The Fab clone HO538-213 (filled circles) was tested for its ability to inhibit HIV-1_{JR-FL} replication at a concentration of 0.1 (left), 1.0 (middle), and 2.5 (right) μg/mL. The CD4 non-reactive Fab clone 13-3 (open circles) was used as a negative control. Representative data from four independent experiments are shown. (B) Activation of the tyrosine kinase signaling cascade by HO538-213 in MOLT-4 cells. The detergent-resistant membrane fraction (arrowhead) was isolated by a membrane floatation assay (MFA) from MOLT-4 cells treated with HO538-213, and phosphotyrosine levels were examined by immunoblotting.

Ab-producing cells from the same donor, namely against nuclear Ag and blood group i-glycolipid, was significantly higher than the other donors (Fig. 1A). In addition, we isolated anti-TNF-α IgG and IgM clones from this donor [16]. Although clinical manifestations of autoimmune disorders were lacking, it is likely that the donor may have an immunological background that generates auto-reactive Ab and tolerates them. Moreover, the donor has been healthy for 29 years, as the CD4-reactive Ab was first isolated, suggesting that such CD4-reactive Ab may not disturb host immunity.

Considering that the IgM-producing B cells we isolated went through positive/negative selection, their original target should not be CD4. It is thus likely that the IgM genes accumulated sHM that resulted in cross-reactivity to CD4 in periphery after B-cell maturation. To better understand the unique immunological features of individuals with CD4-reactive Ab and their auto-reactive Ab repertoire, more human monoclonal self-reactive Ab are needed to analyze both their V-region sequences and cross-reactivities. Our experimental approach might be useful for addressing these issues. Unfortunately, however, we were unable to characterize the CD4-reactive Ab-producing cells, as the oligoclonal cultures of B-LCL were terminated after RNA extraction for our Ig gene cloning strategy. We speculate that B-1 cells could be the source of the CD4-reactive Ab, because B-1 cells produce IgM that often cross-reacts with auto-Ag.

Our genetic data indicated that only a fraction of the CD4-reactive Ab could have some HIV-inhibitory function. It is an open question whether such CD4-reactive HIV-inhibitory Ab may be present in the other healthy individuals, as well as in HIV-seropositive long-term non-progressors.

HIV-inhibitory CD4-reactive Ab are effective against multiple HIV clades, as CD4 is the major HIV receptor for all the viral clades [11]. A clinical trial is being conducted to examine the therapeutic efficacy of a humanized CD4-reactive mAb in patients with HIV infection [8, 12]. Although CD4-reactive Ab can be detected in healthy individuals, safety is always a concern when using self-recognizing Ab as therapeutic drugs. Given that HO538-213 was isolated from a healthy individual and that it recognized a different epitope than Leu-3a, HO538-213 might effectively inhibit HIV without disturbing $CD4^+$ T-cell functions. As noted above, the donor from which the three CD4-reactive IgM Fab were isolated has been healthy for more than 29 years since PBMC collection, suggesting that these Ab may not seriously inhibit $CD4^+$ T-cell functions *in vivo* and thus may be useful in treating HIV infection and other disorders [4].

Concluding remarks

This report provides the first clonal genetic analyses of human monoclonal anti-CD4 Ab. IgM is considered to function in "natural humoral immunity", as it has a relatively low affinity for pathogens and confers natural resistance to infectious agents. However, the pathogen-specific immunity function of IgM has not been demonstrated at a clonal level. Our data suggest that CD4-reactive IgM is present in healthy individuals and can contribute to natural resistance to HIV infection and AIDS progression. This is the first clear demonstration of a natural humoral immunity function of IgM against HIV.

Materials and methods

Functional cloning of heavy and light chain Ab genes

The establishment of Ab-producing cells, cloning of Ig genes encoding V regions, ELISA, and the purification of Fab fragments from *Escherichia coli* have been described previously [16]. The experimental procedure is schematically shown in the Supporting Information Fig. 1. In brief, PBMC from 12 donors, including two healthy individuals and ten individuals with autoimmune disorders, were infected with the B95-8 strain of EBV, and 1×10^4 cells were propagated in 96-well plates. The supernatant was analyzed by ELISA using rhCD4 derived from a baculovirus system (50 ng/well; INTRACELL) as an Ag. Other Ag tested, including viral, bacterial, and auto-Ag, are listed in the Supporting Information Fig. 2. Total cellular RNA was isolated from oligoclonal cell populations positive for anti-CD4 Ab production (RNeasy mini kit, Qiagen). cDNAs were synthesized and amplified by PCR with specific primers for human Ig μ-, γ-, λ-, and κ-chains. Only the μ- and κ-chains were amplified from HO538 and HO702 cultures and cloned into the pFab1-His2 vector, generating bacterial Fab-expression libraries [30]. The pFab libraries were screened for the production of CD4-reactive Fab by ELISA. The Fab fragments were purified using an anti-Fab Ab affinity column. The eluted Fab was dialyzed against PBS and concentrated by centrifugation (VIVASPIN concentrator, Vivascience AG). The purity of the Fab Ab was greater than 95% as determined by SDS-PAGE analysis (data not shown).

Surface plasmon resonance biosensor analysis

Surface plasmon resonance analyses were performed using a BIACORE 3000 (GE Healthcare). The hrCD4 was immobilized onto CM5 sensor chips using standard amine-coupling chemistry. The purified Fab was diluted in a running buffer (10 mM HEPES, 0.15 M NaCL, 3 mM EDTA, surfactant P 20, pH 7.4) to 0.3–20 μg/mL and injected at a rate of 20–30 μL/min. The Fab was allowed to associate and dissociate for 120–270 s.

Cells

B-LCL and 293 T cells were maintained in Roswell Park Memorial Institute (RPMI) 1640 (Sigma) supplemented with 10% fetal bovine serum (Japan Bioserum), penicillin, and streptomycin (Invitrogen). The primary mononuclear cells were maintained in RPMI 1640 supplemented with 10% fetal bovine serum, penicillin, streptomycin, 5 μg/mL plasmocin (InvivoGen), 10 mM HEPES, 5 μg/mL anti-CD3 mAb (OKT3, Janssen Pharmaceutical), 70 U/mL recombinant human IL-2 (Shionogi Pharmaceutical), GlutaMax-I (Invitrogen), insulin–transferrin–selenium-A (Invitrogen), and 10 mM HEPES (Invitrogen). Cells were incubated at 37°C in a humidified 5% CO_2 atmosphere.

Other experimental procedures

Procedures for monitoring HIV-1 replication [31] and membrane floatation assays [32] were described previously. Standard auto-Ab was tested by the clinical laboratory testing service SRL (Tokyo, Japan).

Acknowledgements: The authors thank Hideo Tsukamoto for BIACORE analysis. This work was supported by the Japan Health Science Foundation, the Japanese Ministry of Health, Labor and Welfare (H18-AIDS-W-003 to JK), and the Japanese Ministry of Education, Culture, Sports, Science and Technology (18689014 and 18659136 to JK).

Conflict of interest: The authors declare no financial or commercial conflict of interest.

References

1 Henriksson, G., Manthorpe, R. and Bredberg, A., Antibodies to CD4 in primary Sjogren's syndrome. *Rheumatology (Oxford)* 2000. 39: 142–147.

2 Lenert, P., Lenert, G. and Senecal, J. L., CD4-reactive antibodies in systemic lupus erythematosus. *Hum. Immunol.* 1996. 49: 38–48.

3 Lopalco, L., Magnani, Z., Confetti, C., Brianza, M., Saracco, A., Ferraris, G., Lillo, F. *et al.*, Anti-CD4 antibodies in exposed seronegative adults and in newborns of HIV type 1-seropositive mothers: a follow-up study. *AIDS Res. Hum. Retroviruses* 1999. 15: 1079–1085.

4 Herzog, C., Walker, C., Muller, W., Rieber, P., Reiter, C., Riethmuller, G., Wassmer, P. *et al.*, Anti-CD4 antibody treatment of patients with rheumatoid arthritis: I. Effect on clinical course and circulating T cells. *J. Autoimmun.* 1989. 2: 627–642.

5 Rieber, E. P., Federle, C., Reiter, C., Krauss, S., Gurtler, L., Eberle, J., Deinhardt, F. and Riethmuller, G., The monoclonal CD4 antibody M-T413 inhibits cellular infection with human immunodeficiency virus after viral attachment to the cell membrane: an approach to postexposure prophylaxis. *Proc. Natl. Acad. Sci. USA* 1992. 89: 10792–10796.

6 Bentley, D. L. and Rabbits, T. H., Human immunoglobulin variable region genes – DNA sequences of two V kappa genes and a pseudogene. *Nature* 1980. 288: 730–733.

7 Moir, S., Lapointe, R., Malaspina, A., Ostrowski, M., Cole, C. E., Chun, T. W., Adelsberger, J. *et al.*, CD40-Mediated induction of CD4 and CXCR4 on B lymphocytes correlates with restricted susceptibility to human immunodeficiency virus type 1 infection: potential role of B lymphocytes as a viral reservoir. *J. Virol.* 1999. 73: 7972–7980.

8 Kuritzkes, D. R., Jacobson, J., Powderly, W. G., Godofsky, E., DeJesus, E., Haas, F., Reimann, K. A. *et al.*, Antiretroviral activity of the anti-CD4 monoclonal antibody TNX-355 in patients infected with HIV type 1. *J. Infect. Dis.* 2004. 189: 286–291.

9 Burastero, S. E., Gaffi, D., Lopalco, L., Tambussi, G., Borgonovo, B., De Santis, C., Abecasis, C. *et al.*, Autoantibodies to CD4 in HIV type 1-exposed seronegative individuals. *AIDS Res. Hum. Retroviruses* 1996. 12: 273–280.

10 Boon, L., Holland, B., Gordon, W., Liu, P., Shiau, F., Shanahan, W., Reimann, K. A. and Fung, M., Development of anti-CD4 MAb hu5A8 for treatment of HIV-1 infection: preclinical assessment in non-human primates. *Toxicology* 2002. 172: 191–203.

11 Shearer, M. H., Timanus, D. K., Benton, P. A., Lee, D. R. and Kennedy, R. C., Cross-clade inhibition of human immunodeficiency virus type 1 primary isolates by monoclonal anti-CD4. *J. Infect. Dis.* 1998. 177: 1727–1729.

12 Hurez, V., Kaveri, S. V., Mouhoub, A., Dietrich, G., Mani, J. C., Klatzmann, D. and Kazatchkine, M. D., Anti-CD4 activity of normal human immunoglobulin G for therapeutic use. (Intravenous immunoglobulin, IVIg). *Ther. Immunol.* 1994. 1: 269–277.

13 Bomsel, M., Pastori, C., Tudor, D., Alberti, C., Garcia, S., Ferrari, D., Lazzarin, A. and Lopalco, L., Natural mucosal antibodies reactive with first extracellular loop of CCR5 inhibit HIV-1 transport across human epithelial cells. *AIDS* 2007. 21: 13–22.

14 Sugden, B. and Mark, W., Clonal transformation of adult human leukocytes by Epstein–Barr virus. *J. Virol.* 1977. 23: 503–508.

15 Takekoshi, M., Maeda, F., Tachibana, H., Inoko, H., Kato, S., Takakura, I., Kenjyo, T. *et al.*, Human monoclonal anti-HCMV neutralizing antibody from phage display libraries. *J. Virol. Methods* 1998. 74: 89–98.

16 Takekoshi, M., Maeda, F., Nagatsuka, Y., Aotsuka, S., Ono, Y. and Ihara, S., Cloning and expression of human anti-tumor necrosis factor-alpha monoclonal antibodies from Epstein–Barr virus transformed oligoclonal libraries. *J. Biochem.* 2001. 130: 299–303.

17 Matsuda, F., Ishii, K., Bourvagnet, P., Kuma, K., Hayashida, H., Miyata, T. and Honjo, T., The complete nucleotide sequence of the human immunoglobulin heavy chain variable region locus. *J. Exp. Med.* 1998. 188: 2151–2162.

18 Huber, C., Schable, K. F., Huber, E., Klein, R., Meindl, A., Thiebe, R., Lamm, R. and Zachau, H. G., The V kappa genes of the L regions and the repertoire of V kappa gene sequences in the human germ line. *Eur. J. Immunol.* 1993. 23: 2868–2875.

19 Pech, M. and Zachau, H. G., Immunoglobulin genes of different subgroups are interdigitated within the VK locus. *Nucleic Acids Res.* 1984. 12: 9229–9236.

20 Healey, D., Dianda, L., Moore, J. P., McDougal, J. S., Moore, M. J., Estess, P., Buck, D. *et al.*, Novel anti-CD4 monoclonal antibodies separate human immunodeficiency virus infection and fusion of CD4+ cells from virus binding. *J. Exp. Med.* 1990. 172: 1233–1242.

21 Peterson, A. and Seed, B., Genetic analysis of monoclonal antibody and HIV binding sites on the human lymphocyte antigen CD4. *Cell* 1988. 54: 65–72.

22 Benkirane, M., Hirn, M., Carriere, D. and Devaux, C., Functional epitope analysis of the human CD4 molecule: antibodies that inhibit human immunodeficiency virus type 1 gene expression bind to the immunoglobulin CDR3-like region of CD4. *J. Virol.* 1995. 69: 6898–6903.

23 Sattentau, Q. J., Dalgleish, A. G., Weiss, R. A. and Beverley, P. C., Epitopes of the CD4 antigen and HIV infection. *Science* 1986. 234: 1120–1123.

24 Pal, R., Nair, B. C., Hoke, G. M., Sarngadharan, M. G. and Edidin, M., Lateral diffusion of CD4 on the surface of a human neoplastic T-cell line probed with a fluorescent derivative of the envelope glycoprotein (gp120) of human immunodeficiency virus type 1 (HIV-1). *J. Cell. Physiol.* 1991. 147: 326–332.

25 Finnegan, C. M., Rawat, S. S., Cho, E. H., Guiffre, D. L., Lockett, S., MerrillJr., A. H. and Blumenthal, R., Sphingomyelinase restricts the lateral diffusion of CD4 and inhibits human immunodeficiency virus fusion. *J. Virol.* 2007. 81: 5294–5304.

26 Rawat, S. S., Zimmerman, C., Johnson, B. T., Cho, E., Lockett, S. J., Blumenthal, R. and Puri, A., Restricted lateral mobility of plasma membrane CD4 impairs HIV-1 envelope glycoprotein mediated fusion. *Mol. Membr. Biol.* 2008. 25: 83–94.

27 Xavier, R., Brennan, T., Li, Q., McCormack, C. and Seed, B., Membrane compartmentation is required for efficient T cell activation. *Immunity* 1998. 8: 723–732.

28 Millan, J., Cerny, J., Horejsi, V. and Alonso, M. A., CD4 segregates into specific detergent-resistant T-cell membrane microdomains. *Tissue Antigens* 1999. 53: 33–40.

29 Nguyen, D. H., Giri, B., Collins, G. and Taub, D. D., Dynamic reorganization of chemokine receptors, cholesterol, lipid rafts, and adhesion molecules to sites of CD4 engagement. *Exp. Cell. Res.* 2005. 304: 559–569.

30 Maeda, F., Nagatsuka, Y., Ihara, S., Aotsuka, S., Ono, Y., Inoko, H. and Takekoshi, M., Bacterial expression of a human recombinant monoclonal antibody fab fragment against hepatitis B surface antigen. *J. Med. Virol.* 1999. 58: 338–345.

31 Shimizu, S., Urano, E., Futahashi, Y., Miyauchi, K., Isogai, M., Matsuda, Z., Nohtomi, K. *et al.*, Inhibiting lentiviral replication by HEXIM1, a cellular negative regulator of the CDK9/cyclin T complex. *AIDS* 2007. 21: 575–582.

32 Nagatsuka, Y., Hara-Yokoyama, M., Kasama, T., Takekoshi, M., Maeda, F., Ihara, S., Fujiwara, S. *et al.*, Carbohydrate-dependent signaling from the phosphatidylglucoside-based microdomain induces granulocytic differentiation of HL60 cells. *Proc. Natl. Acad. Sci. USA* 2003. 100: 7454–7459.

Abbreviations: **B-LCL:** B-lymphoblastoid cell lines · **rhCD4:** recombinant human CD4 · **sHM:** somatic hypermutation

Full correspondence: Dr. Jun Komano, AIDS Research Center, National Institute of Infectious Diseases, 1-23-1 Shinjuku, Tokyo 162-864, Japan
Fax: +81-3-5285-1111
e-mail: ajkomano@nih.go.jp

Additional correspondence: Dr. Masataka Takekoshi, Department of Molecular Life Science, Division of Basic Molecular Science and Molecular Medicine, Tokai University School of Medicine, Isehara, Japan
E-mail: mtakekos@is.icc.u-tokai.ac.jp

Received: 2/4/2009
Revised: 22/12/2009
Accepted: 1/2/2010

Dominant-negative derivative of EBNA1 represses EBNA1-mediated transforming gene expression during the acute phase of Epstein–Barr virus infection independent of rapid loss of viral genome

Yumi Kariya,[1,2] Makiko Hamatake,[1] Emiko Urano,[1] Hironori Yoshiyama,[3] Norio Shimizu[2] and Jun Komano[1,4]

[1]AIDS Research Center, National Institute of Infectious Diseases, Tokyo; [2]Department of Virology, Division of Medical Science, Medical Research Institute, Tokyo Medical and Dental University, Tokyo; [3]Research Center for Infection-associated Cancer, Institute for Genetic Medicine, Hokkaido University, Sapporo, Japan

(Received November 1, 2009/Revised November 30, 2009/Accepted December 6, 2009)

The oncogenic human herpes virus, the Epstein–Barr virus (EBV), expresses EBNA1 in almost all forms of viral latency. EBNA1 plays a major role in the maintenance of the viral genome and in the transactivation of viral transforming genes, including EBNA2 and latent membrane protein (LMP-1). However, it is unknown whether inhibition of EBNA1 from the onset of EBV infection disrupts the establishment of EBV's latency and transactivation of the viral oncogenes. To address this, we measured EBV infection kinetics in the B cell lines BALL-1 and BJAB, which stably express a dominant-negative EBNA1 (dnE1) fused to green fluorescent protein (GFP). The EBV genome was surprisingly unstable 1 week post-infection: the average loss rate of EBV DNA from GFP- and GFP-dnE1-expressing cells was 53.4% and 41.0% per cell generation, respectively, which was substantially higher than that of an 'established' *oriP* replicon (2–4%). GFP-dnE1 did not accelerate loss of the EBV genome, suggesting that EBNA1-dependent licensing of the EBV genome occurs infrequently during the acute phase of EBV infection. In the subacute phase, establishment of EBV latency was completely blocked in GFP-dnE1-expressing cells. In contrast, C/W promoter-driven transcription was strongly restricted in GFP-dnE1-expressing cells at 2 days post-infection. These data suggest that inhibition of EBNA1 from the onset of EBV infection is effective in blocking the positive feedback loop in the transactivation of viral transforming genes, and in eradicating the EBV genome during the subacute phase. Our results suggest that gene transduction of GFP-dnE1 could be a promising therapeutic and prophylactic approach toward EBV-associated malignancies. (*Cancer Sci* 2010)

The Epstein–Barr virus (EBV) is a risk factor in several malignant diseases including Burkitt's lymphoma and nasopharyngeal carcinoma.[1–4] The opportunistic B-cell lymphoma is becoming the major cause of death in AIDS patients in an era of highly active antiretroviral therapy (HAART), and EBV is associated with a significant portion of AIDS lymphoma cases.[5,6] Neither an EBV vaccine, nor specific antiviral agents against EBV are available; thus attention should be paid to the development of therapeutic agents against EBV.

EBV-encoded genes including EBNA1, EBNA2, and latent membrane protein (LMP-1) are potential molecular targets for the treatment of EBV-associated lymphomas because they play central roles in the process of malignant transformation.[7] We are interested in EBNA1 since it contributes to EBV oncogenesis in two ways: it supports the maintenance of the EBV genome in *cis* and enhances expression of viral oncogenes, including EBNA2 and LMP-1, in *trans*.[7–9] EBNA1 exerts its biological functions by binding to its cognate binding sites within the family of repeats (FR) and the dyad symmetry element (DS) located within the origin of replication (oriP) of EBV DNA. EBNA1 interacts with FR to enhance transcription from the viral C/W promoters (C/Wp) and to partition EBV DNA to daughter cells; and with DS to initiate DNA replication.[7–9]

Maintenance of the oriP replicon is stable once EBV latency has been established. The loss rate of established oriP plasmids is estimated at 2–4% per cell generation.[10,11] Interestingly, the loss rate of the oriP replicon is significantly higher in cells transiently transduced with oriP plasmids (>25% per cell generation) than in established cells.[12] In primary B cells, EBV DNA is lost rapidly within 2 days post-infection (~98.9%).[13] However, the loss rate of the EBV genome during a week post-infection in B cells remains to be quantified.

Upon EBV infection, the first viral genes expressed are the transactivators EBNA2 and EBNA-LP transcribed from Wp several hours after infection.[7] EBNA2 binds to the EBNA2-responsive elements and, in cooperation with EBNA-LP, enhances transcription from Cp, which leads to expression of all EBNA proteins, including EBNA1. EBNA1 binding to oriP activates C/Wp to boost viral latent gene expression, including the EBNAs and LMP-1. The viral gene transactivation positive feedback loop is established within a few days post-infection, and EBNA1 is one of the key factors that sustain this feedback loop during the acute phase of EBV infection.[14] In parallel, EBNA1 contributes to the establishment of the EBV genome as a licensed replicon. It may be possible to stop EBV infection by breaking the chain of EBNA1-dependent events and thus the EBV-mediated malignant transformation of infected cells. Previous studies have assessed the therapeutic potential of a dominant-negative derivative of EBNA1 (dnE1) in cells in which EBV latency was already established.[15,16] In this study, we critically assessed whether inhibition of EBNA1 limits the early stage of EBV infection in B cells. We provide evidence that expression of dnE1 strongly blocks the expression of virus-encoded oncogenes in acutely infected cells without accelerating EBV genome loss, and disrupts EBV latency in the subacute phase of EBV infection.

Materials and Methods

Cells. The 293T, EBV-negative Burkitt lymphoma cell line BJAB, EBV-positive Burkitt lymphoma cell line Daudi, EBV-transformed healthy donor-derived B lymphoblastoid cell line (B-LCL), and B acute lymphoblastic leukemia cell line BALL-1

[4]To whom correspondence should be addressed.
E-mail: ajkomano@nih.go.jp

doi: 10.1111/j.1349-7006.2009.01474.x

cells (kindly provided by Dr. Yokota, National Institute of Infectious Diseases, Tokyo, Japan) were maintained in RPMI-1640 medium (Sigma, St. Louis, MA, USA) supplemented with 10% fetal bovine serum (Japan Bioserum, Tokyo, Japan), 50 U/mL penicillin, 50 μg/mL streptomycin (Invitrogen, Tokyo, Japan), and incubated at 37°C in a humidified 5% CO_2 atmosphere.

Plasmids. The following primers were used to amplify dnE1 from p1160[17] by PCR: 5′-ACCGGTCTCGAGCAATTGCCA-CCATGCGGGGTCAGGGTGATGGAGG-3′ and 5′-GGATC-CTCGAGCGGCCGCTCACTCCTGCCCTTCCTCACC-3′. The GFP-dnE1 expression vector (pGD) was constructed by cloning the MfeI-XhoI fragment of the PCR product into the BglII-SalI sites of pEGFP-C1 (Clontech, Palo Alto, CA, USA). The MfeI and BglII sites were blunted with T7 RNA polymerase. The AgeI-BamHI fragment from pGD was cloned into the corresponding restriction sites of pCMMP eGFP[15,18] to generate pCMMP GFP-dnE1. The EBNA1 expression vector p1553, the FR-tk-luciferase reporter p985, and pLuciferase (pCMV-luc) have been described previously.[17–20]

Luciferase assay. The 293T cells, grown in 48-well plates, were co-transfected with the indicated plasmids using Lipofectamine 2000 according to the manufacturer's protocol (Invitrogen, Tokyo, Japan). Cells were replated in 96-well plates in triplicate at 2 h post-transfection. Luciferase activity was measured 48 h after transfection using the Steady-Glo Kit (Promega, Madison, WI, USA).

Murine leukemia virus (MLV) vector infection and cell sorting. MLV vectors were produced as described previously.[18] B cells (1×10^7 cells) were incubated with 2 mL of MLV preparation overnight at 4°C with continuous agitation. GFP-positive cells were collected using a FACS sorter (FACS Vantage; Becton Dickinson, San Jose, CA, USA) at 11 days post-infection.

Western blotting. Western blotting was performed as described previously.[21,22] The following reagents were used: anti-GFP (MsX Green Fluorescent Protein; Chemicon, Temecula, CA, USA) and Envision+ Dual Link System-HRP (Dako, Glostrup, Denmark).

EBV infection and nucleic acid extraction. The EBV B95-8 strain was a generous gift from Dr Fujiwara's group at the National Research Institute for Child and Development (Tokyo, Japan). B cells (1×10^7 cells) were incubated with 100 μL of B95-8 EBV for 1 h at 37°C, and genomic DNA was extracted from half of the infected cells soon after infection (QIAamp DNA Mini Kit; Qiagen, Tokyo, Japan). At 15 h post-infection, half of the cells were washed once with PBS and incubated for 5 min in lysis buffer (10 mM Tris-HCl [pH7.4], 10 mM NaCl, 3 mM $MgCl_2$, and 0.5% NP-40). The nuclear fraction was collected by centrifugation for 5 min at 20.6 K × *g* (Kubota 3740; Kubota, Tokyo, Japan), and high molecular weight DNA was extracted (nuclear DNA). At 2 days post-infection and at later time points, high molecular weight DNA, or total RNA (PureLink Total RNA Blood Purification Kit; Invitrogen) was extracted from 1×10^6 or 3×10^6 cells, respectively, according to the manufacturer's protocol. After EBV infection, 10 μM aciclovir (Kayaku, Tokyo, Japan) was added to the culture medium. The production and infection of the recombinant EBV Akata strain carrying GFP and neomycin resistant genes has been described previously.[23] At 2 days post-infection, cells were plated at a density of 1×10^4 cells per well in a flat-bottomed 96-well plate, and cultured in a medium containing 1 mg/mL G418. The efficiency of EBV latency establishment was evaluated as percentage of wells positive for the emergence of G418-resistant cells at 2 to 3 weeks post-G418 selection.

Quantitative real-time PCR. Real-time PCR was performed as described previously; serial dilutions of positive controls were used as standards.[21] Amplifications were performed using the QuantiTect SYBR Green RT-PCR/PCR Kit (Qiagen), and the following primers: BamHI W repeat, 5′-GCCAGAGG-TAAGTGGACTTT-3′ and 5′-AGAAGCATGTATACTAAGC-CTCCC-3′; cyclophilin A (CYPA), 5′-CACCGCCACCATG-GTCAACCCCA-3′ and 5′-CCCGGGCCTCGAGCTTTCGAG-TTGTCCACAGTCAGCAATGG-3′; C/Wp, 5′-CCCTCGGA-CAGCTCCTAAG-3′ and 5′-CTTCACTTCGGTCTCCCCTA-3′; EBER1, 5′-AAAACATGCGGACCACCAGC-3′ and 5′-AG-GACCTACGCTGCCCTAGA-3′. The β-globin primers were described previously.[21] Following PCR amplification, the amplicons were separated in a 2% agarose gel, stained with ethidium bromide, and imaged with a Typhoon scanner (GE Healthcare Bio-Sciences; Piscataway, NJ, USA).

Results

Construction and functional verification of dnE1 fused to GFP. The carboxy half of EBNA1 serves as a functional dominant-negative inhibitor of EBNA1 that restricts the replication and maintenance of oriP plasmids as well as the EBNA1-dependent enhancement of transcription.[17,24] We used a dnE1 mutant encompassing amino acids 377 to 391 (the nuclear localization signal, NLS) and 451 to 641 (the DNA binding and dimerization domain) of EBNA1 (Fig. 1A).[17] To visualize the intracellular distribution of dnE1, we constructed the retroviral expression vector encoding GFP-dnE1. The expression of GFP-dnE1 was verified in transiently transfected 293T cells and stably transduced B cell lines using an MLV vector. To verify the function of GFP-dnE1, we conducted a reporter assay using a plasmid encoding the FR-tk-luciferase cassette. EBNA1 enhances expression of FR-tk-luciferase by binding to FR. If the GFP-dnE1 construct retains dnE1 function, co-expressing EBNA1 and GFP-dnE1 should reduce reporter activity. Luciferase activity was increased significantly upon EBNA1 expression by approximately 5.3-fold, consistent with previous findings (Fig. 1B, $P < 0.05$, two-tailed Student's *t*-test).[17] When GFP-dnE1 was co-expressed, the luciferase activity was decreased. The decrease in luciferase activity was proportional to the increase in GFP-dnE1 expression vector (Fig. 1B, maximum reduction: 22.3%, $P < 0.05$, two-tailed Student's *t*-test). This effect was not observed with GFP alone. In addition, CMV promoter-driven luciferase expression was unaffected by EBNA1, GFP-dnE1, and GFP, suggesting that the reduction in luciferase activity with GFP-dnE1 in the EBNA1/FR-tk-luciferase system is specific. These data indicate that GFP-dnE1 functions as an inhibitor of EBNA1.

Establishment of B cells constitutively expressing GFP-dnE1. To investigate the potential effect of GFP-dnE1 on EBV infection in B cells, we established BALL-1 and BJAB cells, which constitutively express GFP-dnE1, using an MLV vector. GFP was used as a control throughout this study. The distribution of GFP-dnE1 was examined by confocal microscopy, which revealed an even distribution of GFP throughout the cell. In contrast, the majority of GFP-dnE1was localized to the nucleus due to the presence of the NLS (Fig. 2A). Similar observations were made in BJAB and 293T cells (data not shown). We sorted the GFP- or GFP-dnE-expressing cells using a FACS sorter. To test the dose-dependent effect, we collected BALL-1 cell populations bearing high or low levels of GFP fluorescence, denoted as Hi and Lo, respectively. The expression of GFP and GFP-dnE1 was verified by Western blotting, which confirmed that GFP and GFP-dnE1 Hi cells had higher intensity signals than the GFP and GFP-dnE1 Lo cells (Fig. 2B). The rate of cell proliferation and the morphology of GFP-dnE1 cells were indistinguishable from those of GFP cells (Fig. 2A and data not shown).

Effect of GFP-dnE1 on the nuclear translocation of EBV DNA during the acute phase of EBV infection. To assess whether GFP-dnE1 could restrict the nuclear targeting of the EBV

doi: 10.1111/j.1349-7006.2009.01474.x

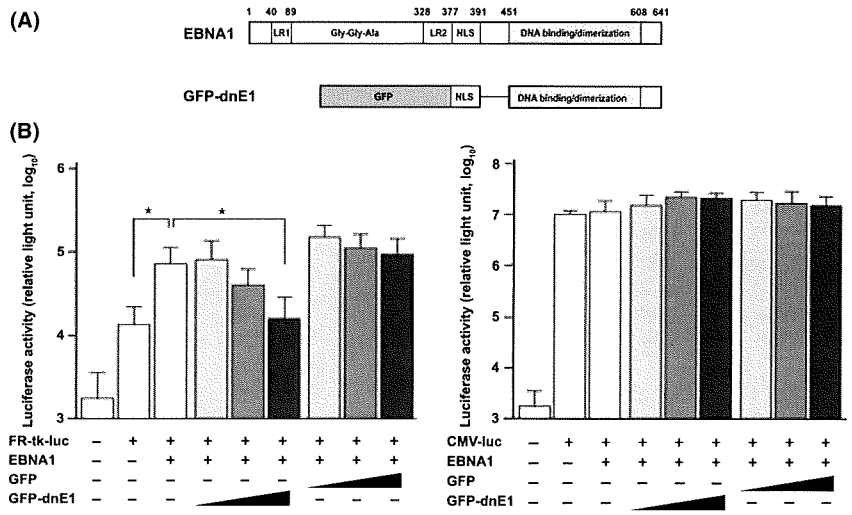

Fig. 1. Construction and functional characterization of a dominant-negative EBNA1 mutant (dnE1) fused to green fluorescent protein (GFP). (A) Structure of the EBNA1 protein and dnE1 used in this study. The linking regions (LR1 and LR2), the Gly-Gly-Ala repeat, the nuclear localization signal (NLS), and the DNA binding and dimerization domain are shown. GFP-dnE1 encodes the NLS and DNA binding and dimerization domain of EBNA1 fused to the C-terminus of GFP. (B) Repression of EBNA1-dependent transcriptional activation by GFP-dnE1. We transfected 293T cells in 48-well plates with 200 ng of FR-tk-luc or CMV-luc reporter, and 500 ng of EBNA1 expression vector, along with increasing amounts of GFP or GFP-dnE1 expression vector (20, 100, and 500 ng, respectively). $*P < 0.05$, two-tailed Student's *t*-test.

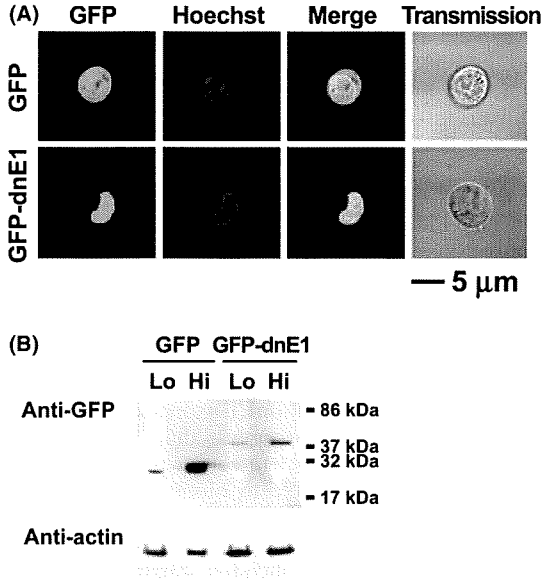

Fig. 2. Verification of stable green fluorescent protein (GFP)-dominant-negative EBNA1 (dnE1) expression in BALL-1 cells. (A) Distribution of GFP and GFP-dnE1 in BALL-1 cells was examined by confocal microscopy. Cells were imaged unfixed using a confocal microscope META 510 (Carl Zeiss, Tokyo, Japan). The green signal represents GFP fluorescence, and blue represents the Hoechst-stained nucleus. The bar represents 5 μm; magnification, ×630. (B) GFP or GFP-dnE1 expression in stably transduced BALL-1 cells was examined by Western blot analysis using an anti-GFP antibody. Protein lysates from 5×10^5 cells were loaded for each sample, except GFP Hi cells (5×10^4). The molecular weight marker is shown on the right.

genome after infection, we measured the amount of EBV DNA recovered from cells immediately after infection (representing the amount of EBV attached to cells) and the amount of EBV DNA that had migrated into the nucleus at 1 day post-infection. We isolated the nuclear fraction to exclude EBV DNA that failed to enter the nucleus. The number of EBV DNA molecules per cell was estimated by real-time PCR, which targeted the BamHI W repeat, in 10 ng of genomic DNA. We estimated the number of EBV DNA per cell given that a single cell contains approximately 10 pg of genomic DNA, and an EBV DNA has 10 copies of BamHI W repeats on average. The nuclear targeting efficiencies of EBV DNA were as follows: BALL-1 GFP cells, 43.3–108.6%; GFP-dnE1 cells, 46.9–65.6%; BJAB GFP cells, 37.4%; GFP-dnE1 cells, 35.0% (Table 1). These data suggested that the effect of GFP-dnE1 on the nuclear targeting of EBV DNA should be assessed more sensitively in BALL-1 and BJAB cell systems than in primary B cells because the nuclear targeting efficiency of EBV DNA in primary B cells is extremely inefficient (~1.1%).[13] In our experimental systems, the nuclear targeting efficiencies of EBV DNA in GFP-dnE1-expressing cells were similar to those in GFP-expressing cells. In addition, the dose-dependency of GFP-dnE1 was not observed in BALL-1 cells (Table 1). These data suggest that the nuclear targeting efficiency of EBV DNA was not restricted by the presence of GFP-dnE1 in B cells upon EBV infection.

Effect of GFP-dnE1 on the rate of loss of EBV DNA during the acute phase of EBV infection. To examine the effect of GFP-dnE1 on the rate of loss (ROL) of EBV DNA during the acute phase of viral infection, we monitored the EBV DNA copy number from day 2 to day 5 or day 6 post-infection, by real-time PCR, which detects the viral genome in both linear and circular configurations (Table 1). The ROL was estimated as the percentage reduction of EBV DNA per cell generation, considering that the cell doubling time is 24 h, and the kinetics of viral genome loss follows an exponential decay. The ROL in GFP-dnE1-expressing cells (19.2–85.9% per cell generation) was similar to GFP-expressing cells (20.5–79.4% per cell generation) in both BALL-1 and BJAB cells. In addition, there was no detectable dose-dependent effect of GFP-dnE1 in BALL-1 cells (Table 1 and Fig. 3). The averages ± SEs of ROL in GFP- and GFP-dnE1-expressing cells from six independent measurements in BALL-1 cells were 37.7 ± 10.7% and 25.7 ± 6.5% per cell generation, respectively (data not shown), which was substantially higher than the rate of loss of an established oriP replicon (2–4%).[10,11] These results reflect the precipitous loss of oriP plas-

Table 1. The kinetics of EBV DNA in the acute phase of EBV infection

Cell	Copy number of EBV DNA per cell at the indicated day†				Nuclear transport (%‡)	Rate of loss of EBV DNA (% per cell generation§)
Expt 1						
BALL-1	Day 0	Day 1	Day 2	Day 5		
GFP Hi	20.38	11.92	3.57	0.01¶	58.5	85.9
GFP Lo	17.26	11.68	3.21	0.56	67.7	44.1
GFP-dnE1 Hi	23.02	10.79	3.30	0.30	46.9	54.9
GFP-dnE1 Lo	18.83	12.36	1.46	0.53	65.6	28.7
BJAB	Day 0	Day 1	Day 2	Day 5		
GFP	155.1	58.8	5.38	0.06	37.4	77.7
GFP-dnE1	64.6	37.4	5.69	0.05	58.0	79.4
Expt 2						
BALL-1	Day 0	Day 1	Day 2	Day 6		
GFP Hi	16.33	17.73	11.10	4.74	108.6	19.2
GFP Lo	17.35	7.51	8.75	1.13	43.3	40.1
GFP-dnE1 Hi	18.46	8.71	8.95	3.38	47.2	21.6
GFP-dnE1 Lo	14.14	7.05	6.97	2.79	49.9	20.5

†Nuclear DNA was used for day 1 data. ‡Estimated from day 0 and day 1 data. §Estimated from day 2 and day 5 or day 6 data with the exponential decay. ¶Below the limit of detection. dnE1, dominant-negative EBNA1; EBV, Epstein–Barr virus; GFP, green fluorescent protein.

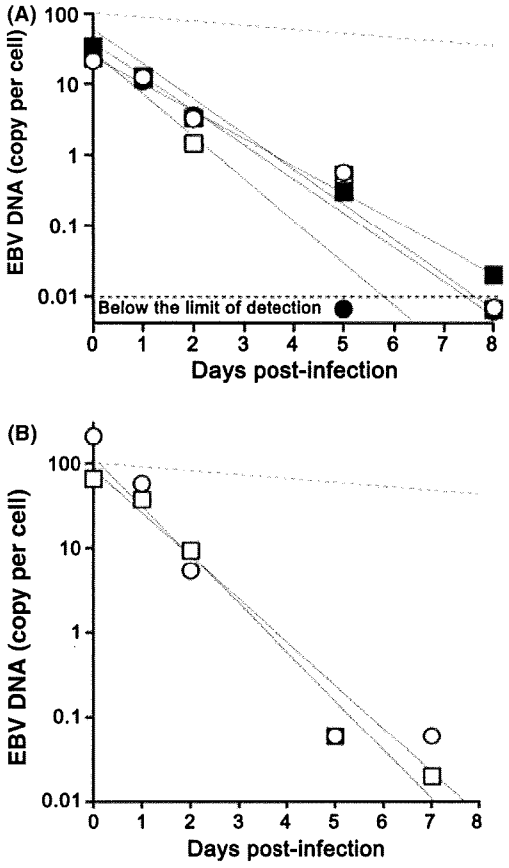

Fig. 3. Kinetics of Epstein–Barr virus (EBV) DNA loss during the acute phase of EBV infection. (A) Representative data from BALL-1 cells (Expt. 1 in Table 1) is shown. The filled squares, open squares, filled circles, and open circles represent GFP Hi, GFP Lo, GFP-dnE1 Hi, and GFP-dnE1 Lo, respectively. The limit of detection was below 0.01 (dashed line). The gray lines represent an approximation to the exponential decay. The dashed gray line represents the 4% rate of loss per cell generation. (B) Representative data from BJAB cells shown in Table 1. The circles and squares represent GFP and GFP-dnE1, respectively. Please see Table 1 for the detailed analysis.

mids (26–37%) in transiently transfected non-B cells.[12] The data suggest that GFP-dnE1 is unable to accelerate the ROL in the acute phase of EBV infection in B cells, presumably because the EBV genome is not established as an EBNA1-dependent stable licensed replicon. It should be noted that this is the first time that quantitative ROL data has been obtained by introducing the oriP replicon into B cells via EBV infection, which is an approach that does not confer any selective advantage on the infected cells.

Effect of GFP-dnE1 on efficiency of establishment of EBV latency. Cells infected with recombinant EBV, carrying the neomycin resistance gene, were seeded at 5×10^3 cells per well into a 96-well plate, and the efficiency of the establishment of EBV latency was assessed as the percentage of wells positive for the emergence of G418-resistant cells. G418-resistant cells appeared in BJAB, Daudi, parental BALL-1, and BALL-1 GFP cells at 56–100% efficiencies. In sharp contrast, G418-resistant cells were absent from GFP-dnE1-expressing BALL-1 cells (Table 2). These data clearly suggest that, although the ROL during the acute phase of EBV infection was not enhanced by GFP-dnE1, GFP-dnE1 was able to block the establishment of EBV latency completely during the subacute phase of EBV infection.

Effect of GFP-dnE1 on EBV-encoded latent gene expression. EBV gene expression was tested at 2 days post-infection by quantitative RT-PCR. We focused on the C/Wp activity because it expresses key viral transactivators including EBNA1, -2, -3s, and -LP to boost viral transforming gene expression. We detected C/Wp-driven transcripts in GFP Hi BALL-1 cells as expected. Conversely, C/Wp-driven transcripts were undetectable in GFP-dnE1 Hi and Lo BALL-1 cells, although these cells retained similar EBV DNA levels to GFP-expressing cells (Fig. 4 and Table 3). The Cp-driven transcript was under the limit of detection by RT-PCR, suggesting that the Wp is predominantly activated at the early phase of EBV infection consistent with previous findings.[7] Inhibition of viral gene transcription was not observed in the RNA polymerase III-driven transcript EBER1,[25] and cyclophilin A mRNA levels were similar between GFP- and GFP-dnE1-expressing cells (Fig. 4 and Table 3). This indicates that the effect of GFP-dnE1 on C/Wp activity is specific, and uncovers an active role of EBNA1 in supporting transactiva-

doi: 10.1111/j.1349-7006.2009.01474.x

Table 2. The establishment efficiency of EBV latency

Cell	Emergence of G418-resistant cells†	
BJAB	100%	(6/6)
Daudi	100%	(10/10)
BALL-1		
Parental	56%	(5/9)
GFP Hi	67%	(2/3)
GFP-dnE1 Hi	0%	(0/6)
GFP-dnE1 Lo	0%	(0/6)

†Percentage of wells positive for G418-resistant cells over the number of tested wells from 96-well plates indicated in the bracket. Shown are the sum of two independent experiments. dnE1, dominant-negative EBNA1; EBV, Epstein–Barr virus; GFP, green fluorescent protein.

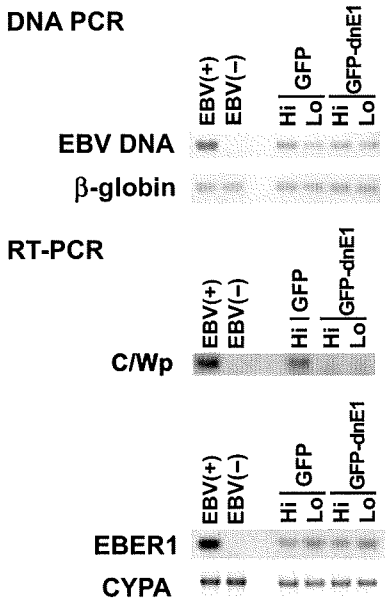

Fig. 4. PCR-based analysis of Epstein–Barr virus (EBV) gene expression. The effect of green fluorescent protein (GFP)-dominant-negative EBNA1 (dnE1) on the loss of EBV DNA (DNA PCR, upper panels) and transcription of the C/W promoter-driven transcript (C/Wp), EBER1, and cyclophilin A (CYPA; RT-PCR, lower panels) in BALL-1 cells at 2 days post-infection were examined. EBV-transformed B-lymphoblastoid cell line (B-LCL) and BJAB cells, denoted as EBV(+) and EBV(–), were used as positive and negative controls for viral DNA and RNA shown, respectively. β-Globin and CYPA were used as controls.

Table 3. Quantification of EBV transcripts in BALL-1 cells by real-time PCR at 2 days post-infection

BALL-1 cells		W1/2 exon (copies†)	EBER1 (copies‡)	CYPA (copies‡)
GFP	Hi	2.2	2.8×10^2	1.4×10^6
	Lo	NT§	0.8×10^2	1.0×10^6
GFP-dnE1	Hi	BLD¶	3.3×10^2	1.3×10^6
	Lo	BLD¶	1.2×10^2	1.5×10^6

†Copies per 13–14 ng total cellular RNA. ‡Copies per 200 ng total cellular RNA. §Not tested. ¶Below the limit of detection. CYPA, cyclophilin A; dnE1, dominant-negative EBNA1; EBV, Epstein–Barr virus; GFP, green fluorescent protein.

tion from C/Wp. Taken together, these results show that inhibition of EBNA1 functions strongly restricts EBV-encoded transforming gene expression and, although there is no detectable effect on the ROL of EBV DNA at the acute phase of viral infection, it blocks the establishment of EBV latency during the subacute phase.

Discussion

This is the first report describing the effect of EBNA1 inhibition from the onset of EBV infection in B cells. Unexpectedly, the dnE1 was unable to accelerate the ROL during the acute phase of EBV infection since dnE1 enhanced the loss of the oriP plasmid in the transient transfection assays.[10,11] In the subacute phase of EBV infection, the establishment of EBV latency was potently blocked by dnE1. In addition, we observed a strong repressive effect of dnE1 on the EBNA1-dependent enhancement of viral gene transcription from C/Wp during the early phase of EBV infection, similar to the transient transfection assays.[17] These data suggest that viral oncogene expression depends heavily on EBNA1 during the acute phase of viral infection, and that EBNA1 contributes little to EBV genome maintenance during this period. The results emphasize that an EBNA1 inhibitor should serve as an attenuator of viral oncogene expression since activation of C/Wp is the 'root' event of the positive feedback loop involved in the transactivation of viral transforming gene expression. In this regard, the EBNA1 inhibition approach could be superior to LMP-1 or EBNA2 inhibition.

If EBNA1 binding to oriP is essential for both the enhancement of viral gene transcription and for genome maintenance, what mechanism prevents dnE1 from affecting the ROL during the acute phase of EBV infection? It is likely that maintenance of the oriP replicon immediately after its introduction into cells is less efficient than in cells harboring an 'established' oriP replicon as an autonomously replicating plasmid. The ROL of an established oriP replicon is 2–4% per cell generation.[10,11] In contrast, our data from the EBV/B cell-based assay gave an average ROL of 26–38% during the week post-infection (acute phase of EBV infection). In agreement with our findings, it is reported that a transiently transduced oriP replicon is lost from cells at 26–37% per cell generation 1–2 weeks post-plasmid transduction.[12] These data indicate that maintenance of the oriP replicon is largely EBNA1-independent immediately after its introduction into cells, regardless of whether the route of introduction is by transfection or EBV infection. In other words, the establishment of EBV latency should be a rare epigenetic event. The data also suggest that the artificial minichromosome approach may be relevant in understanding EBV genome behavior.[12]

Our study suggests that gene therapy using GFP-dnE1 is an attractive approach, not only for therapeutics, but also for prophylactic interventions of EBV-associated malignancies. For example, in peripheral blood stem cell transplantation (PBSCT), GFP-dnE1 transduction into $CD34^+$ cells should protect the differentiated B cells from EBV infection, thus preventing the genesis of EBV-associated B cell lymphomas. We will attempt to prove this hypothesis using a small animal model in future studies.[26] Additionally, EBNA1 is a potential molecular target for developing a small molecular-weight EBV inhibitor as mentioned previously.[14,15] The advantages of EBNA1-inhibitor development are that the biological assay system is already established and the X-ray crystal structure of the DNA-bound EBNA1 DNA binding and dimerization domain is known, which means that computer-aided drug design technology can be immediately applied. Although EBV is associated with various malignancies, preventive and therapeutic measures against EBV infection have not been developed. We believe that an anti-EBV agent, such as an EBNA1 inhibitor, would have an enormous impact in the medical field due to the substantial number of patients with EBV-associated malignancies.

Acknowledgments

We thank Drs Kenichi Imadome and Shigeyoshi Fujiwara for reagents. We also thank Dr Bill Sugden for critically reading the manuscript. This work was supported by the Japan Health Science Foundation, the Ministry of Health, Labor and Welfare of Japan, and the Ministry of Education, Culture, Sports, Science and Technology of Japan.

Disclosure Statement

The authors have no conflict of interest.

References

1 Thompson MP, Kurzrock R. Epstein–Barr virus and cancer. *Clin Cancer Res* 2004; **10**: 803–21.
2 Rickinson AB, Kieff E. Epstin–Barr virus. In: Knipe DM, Howley PM, eds. *Fields Virology*, 5th edn, vol. 2. Philadelphia: Lippincott Williams & Wilkins, 2007; 2655–700.
3 Klein E, Kis LL, Klein G. Epstein–Barr virus infection in humans: from harmless to life endangering virus-lymphocyte interactions. *Oncogene* 2007; **26**: 1297–305.
4 Snow AL, Martinez OM. Epstein–Barr virus: evasive maneuvers in the development of PTLD. *Am J Transplant* 2007; **7**: 271–7.
5 Besson C, Goubar A, Gabarre J *et al.* Changes in AIDS-related lymphoma since the era of highly active antiretroviral therapy. *Blood* 2001; **98**: 2339–44.
6 Carbone A, Cesarman E, Spina M, Gloghini A, Schulz TF. HIV-associated lymphomas and gamma-herpesviruses. *Blood* 2009; **113**: 1213–24.
7 Kieff E, Rickinson AB. Epstin–Barr virus and its replication. In: Knipe DM, Howley PM, eds. *Fields Virology*, 5th edn, vol. 2. Philadelphia: Lippincott Williams & Wilkins, 2007; 2603–54.
8 Lindner SE, Sugden B. The plasmid replicon of Epstein–Barr virus: mechanistic insights into efficient, licensed, extrachromosomal replication in human cells. *Plasmid* 2007; **58**: 1–12.
9 Wang J, Sugden B. Origins of bidirectional replication of Epstein–Barr virus: models for understanding mammalian origins of DNA synthesis. *J Cell Biochem* 2005; **94**: 247–56.
10 Kirchmaier AL, Sugden B. Plasmid maintenance of derivatives of oriP of Epstein–Barr virus. *J Virol* 1995; **69**: 1280–3.
11 Sugden B, Warren N. Plasmid origin of replication of Epstein–Barr virus, oriP, does not limit replication in cis. *Mol Biol Med* 1988; **5**: 85–94.
12 Leight ER, Sugden B. Establishment of an oriP replicon is dependent upon an infrequent, epigenetic event. *Mol Cell Biol* 2001; **21**: 4149–61.
13 Hurley EA, Thorley-Lawson DA. B cell activation and the establishment of Epstein–Barr virus latency. *J Exp Med* 1988; **168**: 2059–75.
14 Altmann M, Pich D, Ruiss R, Wang J, Sugden B, Hammerschmidt W. Transcriptional activation by EBV nuclear antigen 1 is essential for the expression of EBV's transforming genes. *Proc Natl Acad Sci U S A* 2006; **103**: 14188–93.
15 Kennedy G, Komano J, Sugden B. Epstein–Barr virus provides a survival factor to Burkitt's lymphomas. *Proc Natl Acad Sci U S A* 2003; **100**: 14269–74.
16 Nasimuzzaman M, Kuroda M, Dohno S *et al.* Eradication of Epstein–Barr virus episome and associated inhibition of infected tumor cell growth by adenovirus vector-mediated transduction of dominant-negative EBNA1. *Mol Ther* 2005; **11**: 578–90.
17 Kirchmaier AL, Sugden B. Dominant-negative inhibitors of EBNA-1 of Epstein–Barr virus. *J Virol* 1997; **71**: 1766–75.
18 Komano J, Miyauchi K, Matsuda Z, Yamamoto N. Inhibiting the Arp2/3 complex limits infection of both intracellular mature vaccinia virus and primate lentiviruses. *Mol Biol Cell* 2004; **15**: 5197–207.
19 Aiyar A, Sugden B. Fusions between Epstein–Barr viral nuclear antigen-1 of Epstein–Barr virus and the large T-antigen of simian virus 40 replicate their cognate origins. *J Biol Chem* 1998; **273**: 33073–81.
20 Middleton T, Sugden B. EBNA1 can link the enhancer element to the initiator element of the Epstein–Barr virus plasmid origin of DNA replication. *J Virol* 1992; **66**: 489–95.
21 Urano E, Kariya Y, Futahashi Y *et al.* Identification of the P-TEFb complex-interacting domain of Brd4 as an inhibitor of HIV-1 replication by functional cDNA library screening in MT-4 cells. *FEBS Lett* 2008; **582**: 4053–8.
22 Shimizu S, Urano E, Futahashi Y *et al.* Inhibiting lentiviral replication by HEXIM1, a cellular negative regulator of the CDK9/cyclin T complex. *AIDS* 2007; **21**: 575–82.
23 Kanda T, Yajima M, Ahsan N, Tanaka M, Takada K. Production of high-titer Epstein–Barr virus recombinants derived from Akata cells by using a bacterial artificial chromosome system. *J Virol* 2004; **78**: 7004–15.
24 Mackey D, Sugden B. The linking regions of EBNA1 are essential for its support of replication and transcription. *Mol Cell Biol* 1999; **19**: 3349–59.
25 Howe JG, Shu MD. Epstein–Barr virus small RNA (EBER) genes: unique transcription units that combine RNA polymerase II and III promoter elements. *Cell* 1989; **57**: 825–34.
26 Yajima M, Imadome K, Nakagawa A *et al.* A new humanized mouse model of Epstein–Barr virus infection that reproduces persistent infection, lymphoproliferative disorder, and cell-mediated and humoral immune responses. *J Infect Dis* 2008; **198**: 673–82.

doi: 10.1111/j.1349-7006.2009.01474.x

Gene Therapy (2009) 16, 297–302

www.nature.com/gt

SHORT COMMUNICATION

Adenovirus serotype 35 vector-mediated transduction following direct administration into organs of nonhuman primates

F Sakurai[1], S-i Nakamura[2,3,7], K Akitomo[1], H Shibata[2], K Terao[2], K Kawabata[1], T Hayakawa[4,5] and H Mizuguchi[1,6]

[1]*Laboratory of Gene Transfer and Regulation, National Institute of Biomedical Innovation, Ibaraki City, Osaka, Japan;* [2]*Tsukuba Primates Research Center, National Institute of Biomedical Innovation, Tsukuba City, Ibaraki, Japan;* [3]*The Corporation for Production and Research of Laboratory Primates, Tsukuba City, Ibaraki, Japan;* [4]*Pharmaceuticals and Medical Devices Agency, Chiyoda-Ku, Tokyo, Japan;* [5]*Pharmaceutical Research and Technology Institute, Kinki University, Osaka, Japan and* [6]*Graduate School of Pharmaceutical Sciences, Osaka University, Suita City, Osaka, Japan*

Adenovirus (Ad) serotype 35 (Ad35) vectors have attracted remarkable attention as alternatives to conventional Ad serotype 5 (Ad5) vectors. In a previous study, we showed that intravenously administered Ad35 vectors exhibited a safer profile than Ad5 vectors in cynomolgus monkeys, which ubiquitously express CD46, an Ad35 receptor, in a pattern similar to that in humans. However, the Ad35 vectors poorly transduced the organs. In this study, we examined the transduction properties of Ad35 vectors after local administration into organs of cynomolgus monkeys. The vectors transduced different types of cells depending on the organ. Hepatocytes and microglia were mainly transduced after the vectors were injected into the liver and cerebrum, respectively. Injection of the vectors into the femoral muscle resulted in the transduction of cells that appeared to be fibroblasts and/or macrophages. Conjunctival epithelial cells showed transgene expression following infusion into the vitreous body of the eyeball. Transgene expression was limited to areas around the injection points in most of the organs. In contrast, Ad35 vector-mediated transgene expression was not detected in any of the organs not injected with Ad35 vectors. These results suggest that Ad35 vectors are suitable for gene delivery by direct administration to organs.

Gene Therapy (2009) **16,** 297–302; doi:10.1038/gt.2008.154; published online 18 September 2008

Keywords: *adenovirus serotype 35 vector; local administration; nonhuman primate; CD46*

Adenoviruses (Ads) are nonenveloped, double-stranded DNA viruses with icosahedral symmetry. To date, 51 human adenovirus (Ad) serotypes have been identified and classified into six species.[1,2] Among these serotypes, Ad serotype 5 (Ad5), which belongs to species C, is the basis of almost all the Ad vectors commonly used, including those used in clinical trials. Conventional Ad5 vectors have several advantages as gene delivery vehicles. However, it is now well established that the hurdles to Ad5 vector-mediated gene therapy are the high seroprevalence to Ad5 in adults and the refractoriness of cells lacking the expression of coxsackievirus-adenovirus receptor, which is a primary receptor for Ad5, to Ad5 vectors. Pre-existing anti-Ad5 immunity significantly decreases the transduction efficiencies of Ad5 vectors. Even when an Ad5 vector-based vaccine was administered locally into muscle, pre-existing anti-Ad5 antibodies reduced its efficacy.[3,4] A lack of coxsackievirus-adenovirus receptor expression renders the cells unsusceptible to Ad5 vectors at least *in vitro*. Important target cells for gene therapy, including hematopoietic stem cells and dendritic cells, often poorly express coxsackievirus-adenovirus receptor. In addition to these drawbacks, Ad5 vectors have high hepatic tropism. Even when Ad5 vectors are locally injected into a diseased area (for example, a tumor), they are drained from the injection sites into the systemic circulation and primarily transduce hepatocytes because of their high hepatic tropism; on the other hand, efficient transduction is obtained around the injection points. When Ad vectors carry a transgene that exerts cytotoxic effects on transduced cells, Ad vector-mediated hepatic transduction leads to severe hepatotoxicity.[5–7]

In contrast, human species B Ad serotype 35 (Ad35) vectors, which our group and several others have developed,[8–11] possess attractive properties that can overcome the drawbacks of conventional Ad5 vectors. First, Ad35 vector-mediated transduction is not hampered by anti-Ad5 antibodies, because Ad35 belongs to a different species (species B) than Ad5 (species C). Second, Ad35 vectors bind to human CD46 as a receptor.

Correspondence: Dr H Mizuguchi, Laboratory of Gene Transfer and Regulation, National Institute of Biomedical Innovation, 7-6-8 Asagi, Saito, Ibaraki City, Osaka 567-0085, Japan.
E-mail: mizuguch@nibio.go.jp
[7]Current address: Research Center of Animal Life Science, Shiga University of Medical Science, Otsu City, Shiga, Japan.
Received 24 July 2008; revised 24 August 2008; accepted 24 August 2008; published online 18 September 2008

Human CD46 is expressed on almost all human cells, leading to broad tropism of Ad35 vectors in human cells, including coxsackievirus-adenovirus receptor-negative cells.[8,12] However, intravenous administration of Ad35 vectors resulted in inefficient transduction in the organs of human CD46-transgenic (CD46TG) mice and cynomolgus monkeys, which express CD46 in a pattern similar to that of humans.[13–15] These results indicate that CD46 does not successfully serve as a receptor for intravascularly injected Ad35 vectors and that Ad35 vectors are unsuitable for intravascular transduction. However, this property of Ad35 vectors would suggest a potential advantage, in that unwanted transduction would not occur in organs other than the organs targeted following direct injection of Ad35 vectors when draining from injected sites into the bloodstream. These properties suggest that Ad35 vectors would be suitable for gene transfer by local administration into the organs. In this study, we examined the transduction properties of Ad35 vectors following intraorgan administration in nonhuman primates, that is, cynomologus monkeys.

A previously constructed Ad35 vector expressing β-galactosidase (Ad35LacZ)[15] was locally administered at a dose of 1.5×10^{11} vector particles (VP) per point (high dose) or 3×10^{10} VP per point (low dose) in the following eight organs of two cynomolgus monkeys (designated no. 8 and no. 9; no. 8 received the high dose of Ad35LacZ and no. 9 received the low dose): liver, cerebrum, eyeball (vitreous body), quadriceps femoris muscle, pancreas, kidney, spleen and nasal cavity. Four days after administration, the tissues around the injection sites (approximately $40 \times 40 \times 10$ mm^3 with a central focus at the injection point) were collected and subjected to an analysis of β-galactosidase expression and histological pathology. The health condition of the monkeys was also monitored until necropsy.

Overall, both monkeys did well during the experiment. There were no apparent abnormalities in body temperature or heart rate, although no. 8, the high-dose monkey, exhibited slight reductions in blood pressure and body weight. Both monkeys apparently exhibited increased serum levels of aspartate aminotransferase and creatine phosphokinase on days 0–2 after injection. Mild decreases in hemoglobin levels and increases in levels of lactate dehydrogenase and C-reactive protein were also found in both animals. However, these changes were probably due to the operation. The levels of alanine aminotransferase, alkaline phosphatase, albumin, glucose, calcium, chloride and sodium in the serum were mostly within the normal ranges.

After the direct injection of the Ad35 vectors, the transduction profiles were assessed by immunostaining of β-galactosidase in the tissue sections; Table 1 summarizes the results. A detailed transduction profile in each organ is described below.

Liver

Direct injection of Ad35LacZ to the liver caused tissue damage around the injection site (Figures 1a and b). Infiltration of inflammatory cells, necrotic focus and regenerated bile duct epithelial cells were observed. Immunostaining of the liver sections revealed that hepatocytes were mainly transduced with Ad35LacZ in both no. 8 and no. 9 monkeys (Figures 2a and b). A higher level of β-galactosidase was expressed in the liver of no. 8 than in that of no. 9. The transduced cells were predominantly distributed around the injection point (approximately 1×1 mm^2) and were not found outside the periphery of the injection site. β-galactosidase was not expressed in the liver lobes, which were not injected with Ad35LacZ. β-galactosidase-expressing cells were mainly found on the border region between the normal and damaged areas. Direct injection of naked plasmid DNA or Ad5 vectors into mouse liver also resulted in the localized distribution of transgene-expressing cells around the injection points.[16,17] The liver would not allow dispersion of locally injected Ad vectors in the tissue.

Table 1 β-galactosidase expression in the organs following direct injection of Ad35LacZ into organs

	No. 8 (high dose)	*No. 9 (low dose)*
Liver	+++	+
Cerebrum	+++	+
Eyeball	+	–
Femoral muscle	+	+
Pancreas	–	++
Kidney	–	++
Spleen	–	–
Nasal cavity	–	–

+++, strong positive; ++, moderate positive; +, weakly positive; –, negative.

Cerebrum

Ad35LacZ was stereotaxically injected into the left frontal lobe of the cerebrum. After infusion of the high dose of Ad35LacZ, softening of the tissue, which appeared necrotic, was widely observed in the left basal ganglia (Figure 1c). Neutrophils were infiltrated into the necrotic area. In contrast, injection of a low dose of Ad35LacZ resulted in no apparent toxicity, although slight bleeding was found around the artery (Figure 1d). Transduced cells, which appeared to be microglia, were found around the softening regions of both no. 8 and no. 9 animals, although the latter had fewer transduced microglia (Figures 2c and d). There were no β-galactosidase-expressing cells in the right hemisphere of the brain, which was infused with phosphate-buffered saline buffer (data not shown).

Eye

Ad35LacZ was infused into the vitreous body for inoculation into the eyeball. The high dose induced invasion by inflammatory cells, including macrophages and neutrophils, into the ciliary body, iris and retina (Figure 1e). Necrotic changes were also found in all layers of the retina. The low dose caused similar damage to the eyeball. The high dose mediated transduction in the conjunctival epithelial cells (Figure 2e). β-galactosidase expression was not observed in other areas. After injection into the vitreous body, Ad35LacZ might be drained from it and transduce the conjunctival epithelial cells. Bora *et al.*[18] demonstrated that human CD46 was hardly expressed in eye tissues, suggesting that these tissues are refractory to Ad35 vectors. We did not find β-galactosidase expression in the eye of no. 9 animal. Phosphate-buffered saline injection did not result in

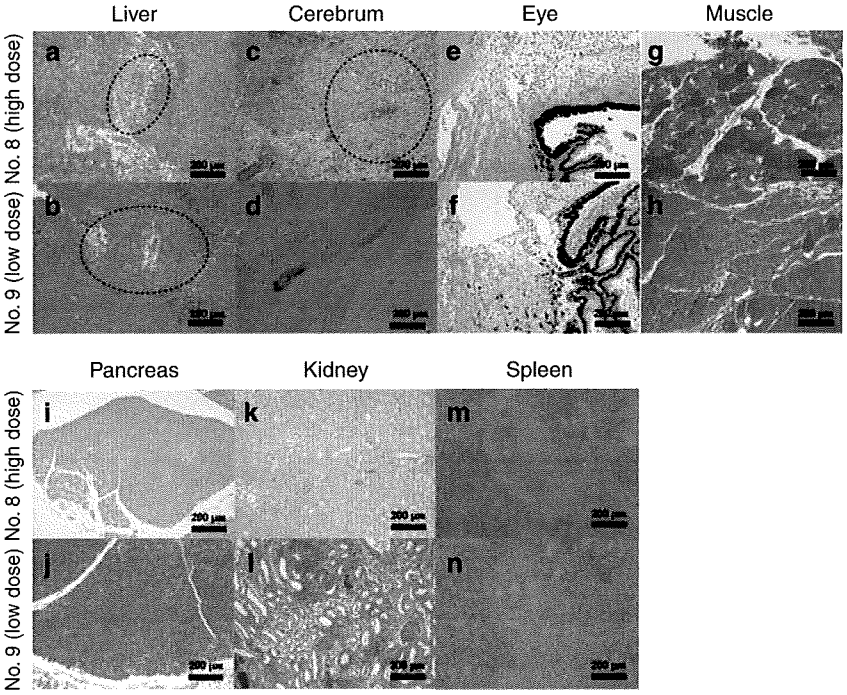

Figure 1 Tissue histology in the organs of cynomolgus monkeys 4 days after intraorgan injection of Ad35LacZ. (**a** and **b**) The liver, (**c** and **d**) cerebrum, (**e** and **f**) eyeball, (**g** and **h**) skeletal muscle, (**i** and **j**) pancreas, (**k** and **l**) kidney and (**m** and **n**) spleen. Young male cynomolgus monkeys (*Macaca fascicularis*) were housed and handled in accordance with the rules for animal care and management of the Tsukuba Primate Center and with the guiding principles for animal experiments using nonhuman primates formulated by the Primate Society of Japan. The animals (approximately 3 years of age, 1.9 and 2.2 kg) were certified free of intestinal parasites and seronegative for simian type-D retrovirus, herpesvirus B, varicella-zoster-like virus and measles virus. The protocol of the experimental procedures was approved by the Animal Welfare and Animal Care Committee of the National Institute of Biomedical Innovation (Osaka, Japan). The liver, cerebrum, eyeball, nasal cavity, pancreas, kidney, skeletal muscle and spleen of cynomolgus monkeys were each injected with Ad35LacZ suspended in 200 µl (100 µl for eyeball) of phosphate-buffered saline at a dose of 1.5×10^{11} vector particles (VP) per point (monkey no. 8) or 3×10^{10} VP per point (monkey no. 9). Four days after injection, tissue sections were hematoxylin–eosin stained by a routine method. Dotted-line circles in (**b**) and (**c**) indicate the necrotic area in the liver and the softening area in the cerebrum, respectively.

transgene expression or apparent abnormality in the eyeball (data not shown).

Femoral muscle

Severe inflammation did not occur after intramuscular injection of the high dose, although we found slight damage to the muscle fibers (Figure 1g). In contrast, the low dose induced more severe inflammation (Figure 1h). Infiltration of neutrophils and macrophages was seen in the muscle of no. 9. It is currently unclear why the low dose induced higher levels of damage. A slight difference in the injection point might affect Ad35 vector-induced inflammatory responses in the muscle. β-galactosidase expression was found only in the cells that appeared to be macrophages and/or fibroblasts located among the muscle fibers in both monkeys (Figures 2g and h). No muscle fibers expressed β-galactosidase in either monkey. It remains to be elucidated why intramuscular injection of Ad35 vectors mediated poor transduction in muscle fibers of cynomolgus monkeys. Ad35 vectors transduced the muscle following intramuscular injection in wild-type mice and in CD46TG mice.[12,14] The transduction mechanism and efficiencies of Ad35 vectors in muscle fibers might differ among species, and the muscle of nonhuman primates might be more refractory to transduction than that of rodents. Thirion *et al.*[19] demonstrated that Ad vectors would transduce human, rat and mouse primary muscle cells through different pathways. Danko *et al.*[20] reported that transgene expression levels by intramuscular injection of naked DNA were lower in dogs and nonhuman primates than in rodents. On the other hand, several studies demonstrated the utility of Ad35 vectors as vaccine vectors that express antigen by intramuscular administration in mice and nonhuman primates.[3,4] Macrophages and/or dendritic cells transduced with Ad35 vectors might play important roles in transgene-specific immune responses by intramuscular injection of Ad35 vectors.

Pancreas

Injection into the pancreas caused no severe damage to that organ in either monkey (Figures 1i and j). We did not find transduced cells in the pancreas of no. 8; in contrast, β-galactosidase was apparently expressed in exocrine acinar cells of no. 9 in the pancreatic lobules (Figures 2i and j). Chemiluminescence assay of β-galactosidase also revealed significant levels of β-galactosidase expression in the pancreas of no. 9 but not in that of no. 8 (data not shown). Wang *et al.*[21] also demonstrated that direct injection of conventional Ad vectors and adenoassociated virus vectors into murine pancreas achieved efficient transduction in acinar cells. Pancreatic acinar cells would be susceptible to Ad vectors.

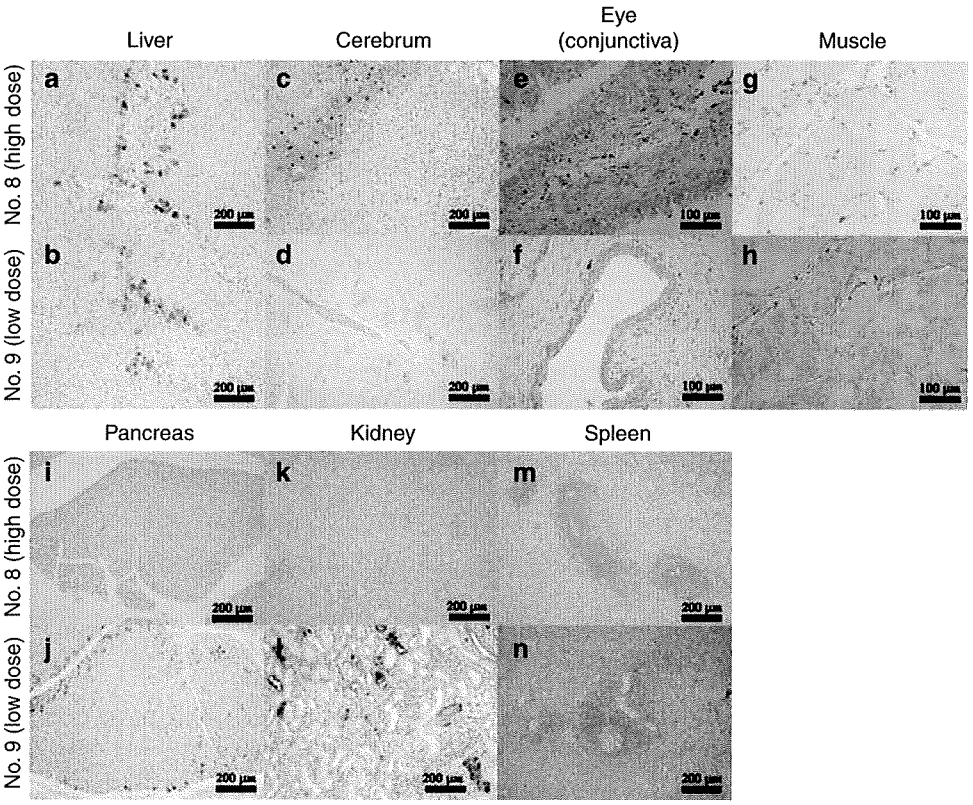

Figure 2 β-galactosidase expression in the organs of cynomolgus monkeys 4 days after intraorgan injection of Ad35LacZ. (**a** and **b**) The liver, (**c** and **d**) cerebrum, (**e** and **f**) eyeball, (**g** and **h**) skeletal muscle, (**i** and **j**) pancreas, (**k** and **l**) kidney and (**m** and **n**) spleen. Ad35LacZ was locally administered in the organs of cynomolgus monkeys at the low (3×10^{10} vector particles (VP) per point) or high dose (1.5×10^{11} VP per points) as described in Figure 1. Four days after injection, the tissues were collected for analysis of β-galactosidase expression and histological pathology. Immunostaining of β-galactosidase was performed using anti-β-galactosidase antibody (Abcam, Cambridge, UK).

Kidney

Ad35LacZ injection to the left kidney induced infiltration by inflammatory cells, including lymphocytes, into the interstitial tissue of the kidney (Figures 1k and l). The right kidney, which was injected with phosphate-buffered saline, did not exhibit β-galactosidase expression or inflammatory responses (data not shown). The high dose did not mediate β-galactosidase expression, but the low dose led to apparent transduction (Figures 2k and l). The renal tubular epithelial cells were mainly transduced with Ad35LacZ. In the kidney, compared with the other organs, transduced cells were more widely spread around the injection points. Refractoriness to the high dose and massive β-galactosidase expression by the low dose in the pancreas and kidney together form a major conundrum in this study. The differences in transduction efficiencies might be due to the slight differences in injection sites. Especially, Ad35LacZ may have been drained into the renal tubule of no. 9 following injection into the kidney, leading to efficient transduction in the renal tubule epithelial cells. Ad35 was originally identified in the kidney and causes cystitis,[22] indicating the tropism of Ad35 for renal epithelial cells.

Spleen and nasal cavity

Unexpectedly, direct injection of Ad35LacZ to the spleen did not induce inflammatory responses such as hyperplasia (Figures 1m and n). There was no β-galactosidase expression in the spleen of either monkey (Figures 2m and n). For transduction in the mucosal membrane of the nasal cavity, Ad35 vector suspensions were instilled into the nasal cavity of each monkey, but neither one showed β-galactosidase expression or cellular damage in the mucosal membrane of the nasal cavity (data not shown).

Other organs

β-galactosidase production in the lung, heart, thymus, bone marrow, lymph node, bladder and testis, which were not injected with Ad35LacZ, were examined by chemiluminescence assay. None of these organs showed detectable β-galactosidase expression (data not shown).

Next, we determined the blood concentrations of Ad35LacZ genome DNA in the blood using quantitative real-time PCR to examine whether or not Ad35LacZ locally injected to the organs was drained from the injection site into the bloodstream. The Ad35 vector DNA was detected in the blood as soon as 6 h post-injection, then gradually decreased (Figure 3). However, the blood-clearance kinetics of Ad35LacZ following intraorgan injection were slower than those following intravenous administration, which were previously reported,[23] although the total amounts of Ad35 vector doses in this study (no. 8: 1.5×10^{11} VP $\times$ 8 points; no. 9: 3×10^{10} VP $\times$ 8 points) were comparable to or lower than those in the previous study in which Ad35LacZ was intravenously infused in cynomolgus monkeys ($0.4–2 \times 10^{12}$ VP per kg, 1.88–2.96 kg).[23] Ad35 vector

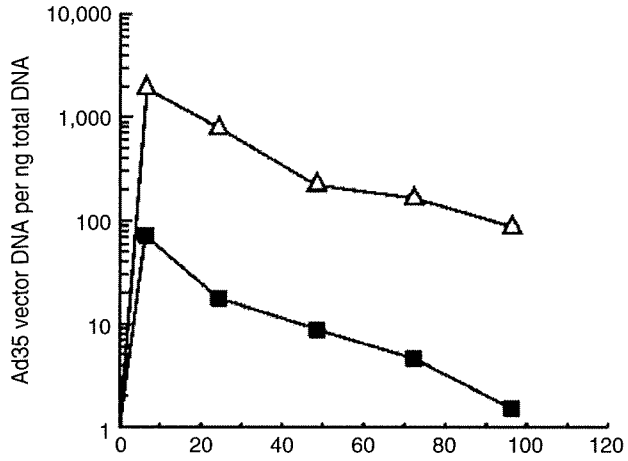

Figure 3 Blood concentrations of Ad35 vectors in cynomolgus monkeys following intraorgan administration. Ad35LacZ was locally administered in the organs of cynomolgus monkeys at the low (3×10^{10} vector particles (VP) per point, closed square) or high dose (1.5×10^{11} VP per points, open triangle) as described in Figure 1. Blood was collected at the indicated post-injection time points (6, 24, 48, 72 and 96 h post-injection). Total DNA, including Ad vector DNA, was isolated from the blood, and the Ad vector DNA contents were measured by quantitative TaqMan PCR assay, as previously described.[23]

DNA was still detectable 4 days after injection. These results suggest that Ad35 vectors or Ad35 vector DNA remaining in the injection sites might be gradually released from the injection sites and drained into the bloodstream.

Furthermore, to examine whether or not Ad35LacZ draining into the bloodstream was accumulated in the organs, we determined the Ad35 DNA contents in the portions of the liver and spleen that were away from the respective injection sites. The liver and spleen play crucial roles in the clearance of systemically injected Ad vectors. The Ad35 vector DNA was not detected in those portions of the liver in no. 9, but was detected in the portions of the liver in no. 8 and in those of the spleen in both monkeys (data not shown). These results suggest that Ad35LacZ or the Ad35 vector DNA draining into the systemic circulation would be taken up by the liver and spleen. We further assessed the Ad35 DNA contents in the lungs, heart, thymus and bone marrow, in which Ad35 vectors were not directly infused. Ad35 vector DNA was detected in the lungs and heart of no. 8 but not in those of no. 9 (data not shown). We did not detect Ad35 vector DNA in the thymus or bone marrow of either monkey. Considering that intravascularly injected Ad35 vectors did not efficiently transduce organs,[15] organs must not be transduced with Ad35LacZ, which is drained into the bloodstream and taken up by the organs.

In most cases of cancer gene therapy using Ad vectors, the vectors are administered directly to the tumor regions.[24–26] When used as vaccine vectors, on the other hand, Ad vectors are intramuscularly injected.[27,28] In addition, Ad vectors are intramyocardially injected in angiogenic gene therapy.[29,30] Thus, direct infusion of Ad vectors to organs is one of the most frequent application methods in clinical settings. However, there has been little information about the transduction properties of these vectors following direct injection into organs. This study demonstrated that different types of cells were transduced with Ad35 vectors depending on the organ after direct infusion into the organ. The differences in the histological structures and cell types comprising the organs would explain the differences in transduction properties of locally injected Ad35 vectors. This study provides important information for clinical study by intraorgan injection of Ad35 vectors, although the characteristics of the organs (structure, cell types and so on) differ different between normal tissue and diseased areas.

Acknowledgements

We thank Fumiko Ono and Chieko Ohno (The Corporation for Production and Research of Laboratory Primates, Ibaraki, Japan) for their help. This study was supported by grants from the Ministry of Health, Labour, and Welfare of Japan and by a Grant-in-Aid for Scientific Research (B) from the Ministry of Education, Culture, Sports, Science, and Technology (MEXT) of Japan.

References

1 Havenga MJ, Lemckert AA, Ophorst OJ, van Meijer M, Germeraad WT, Grimbergen J *et al.* Exploiting the natural diversity in adenovirus tropism for therapy and prevention of disease. *J Virol* 2002; **76**: 4612–4620.
2 De Jong JC, Wermenbol AG, Verweij-Uijterwaal MW, Slaterus KW, Wertheim-Van Dillen P, Van Doornum GJ *et al.* Adenoviruses from human immunodeficiency virus-infected individuals, including two strains that represent new candidate serotypes Ad50 and Ad51 of species B1 and D, respectively. *J Clin Microbiol* 1999; **37**: 3940–3945.
3 Lemckert AA, Sumida SM, Holterman L, Vogels R, Truitt DM, Lynch DM *et al.* Immunogenicity of heterologous prime-boost regimens involving recombinant adenovirus serotype 11 (Ad11) and Ad35 vaccine vectors in the presence of anti-ad5 immunity. *J Virol* 2005; **79**: 9694–9701.
4 Nanda A, Lynch DM, Goudsmit J, Lemckert AA, Ewald BA, Sumida SM *et al.* Immunogenicity of recombinant fiber-chimeric adenovirus serotype 35 vector-based vaccines in mice and rhesus monkeys. *J Virol* 2005; **79**: 14161–14168.
5 Mizuguchi H, Hayakawa T. Enhanced antitumor effect and reduced vector dissemination with fiber-modified adenovirus vectors expressing herpes simplex virus thymidine kinase. *Cancer Gene Ther* 2002; **9**: 236–242.
6 Okada Y, Okada N, Mizuguchi H, Hayakawa T, Mayumi T, Mizuno N. An investigation of adverse effects caused by the injection of high-dose TNFalpha-expressing adenovirus vector into established murine melanoma. *Gene Therapy* 2003; **10**: 700–705.
7 Suzuki T, Sakurai F, Nakamura S, Kouyama E, Kawabata K, Kondoh M *et al.* miR-122a-regulated expression of a suicide gene prevents hepatotoxicity without disturbing the antitumor effects in suicide gene therapy. *Mol Ther* 2008, (in press).
8 Sakurai F, Mizuguchi H, Hayakawa T. Efficient gene transfer into human CD34+ cells by an adenovirus type 35 vector. *Gene Therapy* 2003; **10**: 1041–1048.
9 Vogels R, Zuijdgeest D, van Rijnsoever R, Hartkoorn E, Damen I, de Bethune MP *et al.* Replication-deficient human adenovirus type 35 vectors for gene transfer and vaccination: efficient human cell infection and bypass of preexisting adenovirus immunity. *J Virol* 2003; **77**: 8263–8271.

10 Gao W, Robbins PD, Gambotto A. Human adenovirus type 35: nucleotide sequence and vector development. *Gene Therapy* 2003; **10**: 1941–1949.
11 Seshidhar Reddy P, Ganesh S, Limbach MP, Brann T, Pinkstaff A, Kaloss M *et al*. Development of adenovirus serotype 35 as a gene transfer vector. *Virology* 2003; **311**: 384–393.
12 Sakurai F, Mizuguchi H, Yamaguchi T, Hayakawa T. Characterization of *in vitro* and *in vivo* gene transfer properties of adenovirus serotype 35 vector. *Mol Ther* 2003; **8**: 813–821.
13 Sakurai F, Kawabata K, Koizumi N, Inoue N, Okabe M, Yamaguchi T *et al*. Adenovirus serotype 35 vector-mediated transduction into human CD46-transgenic mice. *Gene Therapy* 2006; **13**: 1118–1126.
14 Verhaagh S, de Jong E, Goudsmit J, Lecollinet S, Gillissen G, de Vries M *et al*. Human CD46-transgenic mice in studies involving replication-incompetent adenoviral type 35 vectors. *J Gen Virol* 2006; **87**: 255–265.
15 Sakurai F, Nakamura S, Akitomo K, Shibata H, Terao K, Kawabata K *et al*. Transduction properties of adenovirus serotype 35 vectors after intravenous administration into nonhuman primates. *Mol Ther* 2008; **16**: 726–733.
16 Sakai M, Nishikawa M, Thanaketpaisarn O, Yamashita F, Hashida M. Hepatocyte-targeted gene transfer by combination of vascularly delivered plasmid DNA and *in vivo* electroporation. *Gene Therapy* 2005; **12**: 607–616.
17 Crettaz J, Berraondo P, Mauleon I, Ochoa L, Shankar V, Barajas M *et al*. Intrahepatic injection of adenovirus reduces inflammation and increases gene transfer and therapeutic effect in mice. *Hepatology* 2006; **44**: 623–632.
18 Bora NS, Gobleman CL, Atkinson JP, Pepose JS, Kaplan HJ. Differential expression of the complement regulatory proteins in the human eye. *Invest Ophthalmol Vis Sci* 1993; **34**: 3579–3584.
19 Thirion C, Lochmuller H, Ruzsics Z, Boelhauve M, Konig C, Thedieck C *et al*. Adenovirus vectors based on human adenovirus type 19a have high potential for human muscle-directed gene therapy. *Hum Gene Ther* 2006; **17**: 193–205.
20 Danko I, Williams P, Herweijer H, Zhang G, Latendresse JS, Bock I *et al*. High expression of naked plasmid DNA in muscles of young rodents. *Hum Mol Genet* 1997; **6**: 1435–1443.
21 Wang AY, Peng PD, Ehrhardt A, Storm TA, Kay MA. Comparison of adenoviral and adeno-associated viral vectors for pancreatic gene delivery *in vivo*. *Hum Gene Ther* 2004; **15**: 405–413.
22 Hierholzer JC. Adenoviruses in the immunocompromised host. *Clin Microbiol Rev* 1992; **5**: 262–274.
23 Sakurai F, Nakamura S, Akitomo K, Shibata H, Terao K, Hayakawa T *et al*. Transduction properties of adenovirus serotype 35 vectors after intravenous administration in non-human primates. *Mol Ther* 2008; **16**: 726–733.
24 Shirakawa T, Terao S, Hinata N, Tanaka K, Takenaka A, Hara I *et al*. Long-term outcome of phase I/II clinical trial of Ad-OC-TK/VAL gene therapy for hormone-refractory metastatic prostate cancer. *Hum Gene Ther* 2007; **18**: 1225–1232.
25 Shimada H, Matsubara H, Shiratori T, Shimizu T, Miyazaki S, Okazumi S *et al*. Phase I/II adenoviral p53 gene therapy for chemoradiation resistant advanced esophageal squamous cell carcinoma. *Cancer Sci* 2006; **97**: 554–561.
26 Tong AW, Nemunaitis J, Su D, Zhang Y, Cunningham C, Senzer N *et al*. Intratumoral injection of INGN 241, a nonreplicating adenovector expressing the melanoma-differentiation associated gene-7 (mda-7/IL24): biologic outcome in advanced cancer patients. *Mol Ther* 2005; **11**: 160–172.
27 Catanzaro AT, Koup RA, Roederer M, Bailer RT, Enama ME, Moodie Z *et al*. Phase 1 safety and immunogenicity evaluation of a multiclade HIV-1 candidate vaccine delivered by a replication-defective recombinant adenovirus vector. *J Infect Dis* 2006; **194**: 1638–1649.
28 Rosenberg SA, Zhai Y, Yang JC, Schwartzentruber DJ, Hwu P, Marincola FM *et al*. Immunizing patients with metastatic melanoma using recombinant adenoviruses encoding MART-1 or gp100 melanoma antigens. *J Natl Cancer Inst* 1998; **90**: 1894–1900.
29 Stewart DJ, Hilton JD, Arnold JM, Gregoire J, Rivard A, Archer SL *et al*. Angiogenic gene therapy in patients with nonrevascularizable ischemic heart disease: a phase 2 randomized, controlled trial of AdVEGF(121) (AdVEGF121) versus maximum medical treatment. *Gene Therapy* 2006; **13**: 1503–1511.
30 Rosengart TK, Lee LY, Patel SR, Kligfield PD, Okin PM, Hackett NR *et al*. Six-month assessment of a phase I trial of angiogenic gene therapy for the treatment of coronary artery disease using direct intramyocardial administration of an adenovirus vector expressing the VEGF121 cDNA. *Ann Surg* 1999; **230**: 466–470; discussion 470–472.